

An-Najah National University
Faculty of Graduate Studies

**Synthesis of Nano-Sized Cobalt oxide Nano-Particles
Stabilized in Surfactant and Polymer Matrix and their
Magnetic Properties**

By
Fadi Mohammad Mostafa Naalweh

Supervisor
Dr. Sharif Musameh
Co-Supervisor
Dr. Mohammed Suleiman

**This Thesis is submitted in Partial Fulfillment of Requirements for the
Degree of Master of Physics, Faculty of Graduate Studies An-Najah
National University Nablus, Palestine.**
2013

**Synthesis of Nano-Sized Cobalt oxide Nano-Particles
Stabilized in Surfactant and Polymer Matrix and their
Magnetic Properties**

By

Fadi Mohammad Mostafa Naalweh

This thesis was defended successfully on 09 /05/2013, and approved by:

Defense Committee Members

Signature

Dr. Sharif Musameh

(Supervisor)



Dr. Mohammed Suleiman

(Co-Supervisor)



Dr. Abdel-Rahman Abu-Labdeh (External Examiner)



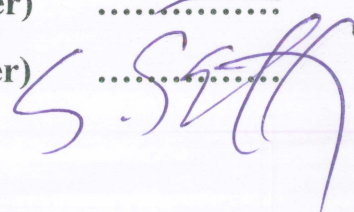
Prof. Issam Rashid

(Internal Examiner)



Prof. Ghassan Saffarini

(Internal Examiner)



Acknowledgments

I dedicate this thesis to my lovely parents, brothers, sisters, relatives, and my family.

I would like to express my gratitude to my supervisors, Dr. Sharif Musameh, and Dr. Mohammed Suleiman, for their expertise, understanding and patience.

I warmly thank everybody who offered great help and efforts which enabled me to complete this thesis.

الإقرار

أنا الموقع أدناه مقدم الرسالة التي تحمل عنوان:

**Synthesis of Nano-Sized Cobalt oxide Nano-Particles
Stabilized in Surfactant and Polymer Matrix and their
Magnetic Properties**

تحضير عينات من أكاسيد الكوبالت على شكل جزيئات نانوية ودراسة خصائصها
المغناطيسية

أقر بأن ما اشتملت عليه هذه الرسالة إنما هو من نتاج جهدي الخاص ، باستثناء ما تمت الإشارة إليه حيثما ورد ، وان هذه الرسالة ككل من أو جزء منها لم يقدم من قبل لنيل أية درجة أو بحث علمي أو بحثي لدى أية مؤسسة تعليمية أو بحثية أخرى.

Declaration

The work provided in this thesis, unless otherwise referenced, is the researcher's own work, and has not been submitted elsewhere for any other degree or qualification.

Student's name:

اسم الطالب:

Signature:

التوقيع:

Date:

التاريخ:

List of Abbreviations

Hexagonal Closed Pack	HCP
Anodized Aluminum Oxide	AAO
Scanning Electron Microscopy	SEM
Transmission Electron Microscopy	TEM
X-ray Diffraction Analysis	XRD
Vibrating Sample Magnetometer	VSM
Filed Emission Scanning Electron Microscopy	FE-SEM
Fourier Transforms Infrared Spectroscopy	FT-IR
Magnetic Saturation	M_s
High Coercivity	H_c
A positive Test Charge	Q
Magnetic Force	F
Magnetic Field	H
Magnetic Induction (Flux)	B
Magnetic Dipole Moment	m
Magnetization	M
Magnetic Susceptibility	χ_m
Permeability of Free Space	μ_o
Centimeter Gram Second System	cgs
Permeability	μ
Curie Constant	C
Critical Temperature	θ
Saturation Flux Density	B_s
Remanence Point	M_r
Cobalt(II) Chloride Hexahydrate	$CoCl_2 \cdot 6H_2O$
Sodium Hydroxide	$NaOH$
Polyvinylpyrrolidone	PVP
Tetraoctylammonium Bromide	$TOAB$
Lanthanum Hexaborid	LaB_6
Field Emission Gun	FEG
Energy Dispersive X-ray Spectroscopy	EDS/EDX
Revolutions Per Minute	rpm
Infrared	IR

List of Contents

No.	Subject	Page
	Acknowledgements	III
	Declaration	IV
	List of Abbreviations	V
	List of Contents	VI
	List of Tables	VIII
	List of Figures	IX
	Abstract	XI
	Chapter 1 : Introduction	2
1.1	Literature Review	4
1.2	Objectives	6
	Chapter 2 : Theoretical Background	9
2.1	Magnetization	9
2.3	Relation Between B, H, and M	9
2.4	Magnetic Susceptibility χ_m	10
2.5	Diamagnetism	13
2.6	Paramagnetism	14
2.7	Ferromagnetism	14
2.8	Antiferromagnetism	15
2.9	Ferrimagnetism	15
2.10	Superparamagnetism	16
	Chapter 3 : Experimental Work	20
3.1	Experimental Equipment and Tools	20
3.1.1	FT-IR Spectroscopy	20
3.1.2	Scanning Electron Microscopy	21
3.1.3	Energy Dispersive X-ray Spectroscopy	22
3.2	Chemicals and Components	23
3.3	Sample Preparation	23
3.3.1	Salt Reduction Method Without Any Stabilizer	24
3.3.2	Salt Reduction Method in the Presence of PVP Stabilizer	25
3.3.3	Salt Reduction Method in the Presence of TOAB Stabilizer	25
	Chapter 4 : Results and Discussion	27
4.1	Sample Characterization	27
4.1.1	FT-IR Spectroscopy	27
4.1.2	EDS Measurements	31
4.1.3	SEM Measurements	32
4.1.4	VSM Magnetic Measurements	37
4.2	Conclusion	42

VII

4.3	Future Work	43
	References	44
	Appendices	50
	المخلص	ب

List of Tables

No.	Table	Page
Table 4.1	The samples with the conditions in which they were prepared.	27
Table 4.2	The size of the samples at different temperatures.	36

List of Figures

No.	Figure	Page
Figure 2.1	Alignments of magnetic dipole moment at room temperature in zero applied-field.	11
Figure 2.2	Temperature dependence of the magnetic susceptibility for (a) diamagnetic, (b) paramagnetic, (c) ferromagnetic, and (d) antiferromagnetic materials.	11
Figure 2.3	The atomic dipole configuration with and without a magnetic field for a diamagnetic material.	14
Figure 3.1	Fourier Transform Infra-Red Spectroscopy	20
Figure 3.2	Scanning Electron Microscopy (SEM).	21
Figure 3.3	Schematic diagram of an energy dispersive X-ray spectroscopy system.	22
Figure 3.4	Vibrating Sample Magnetometer (VSM).	23
Figure 3.5	Schematic of preparing samples by the salt reduction method	24
Figure 4.1	FT-IR spectrum of the transmittance versus wavenumber for sample 1.	28
Figure 4.2	FT-IR spectrum of the transmittance versus wavenumber for sample 2.	28
Figure 4.3	FT-IR spectrum of the transmittance versus wavenumber for sample 3.	29
Figure 4.4	FT-IR spectrum of the transmittance versus wavenumber for sample 4.	30
Figure 4.5	FT-IR spectrum of the transmittance versus wavenumber for sample 5.	30
Figure 4.6	EDS measurement for sample 2.	31
Figure 4.7	SEM for Sample 1.	32
Figure 4.8	SEM for Sample 2.	33
Figure 4.9	SEM for Sample 3.	34
Figure 4.10	SEM for Sample 4.	34
Figure 4.11	SEM for Sample 5.	35
Figure 4.12	The magnetization curve at room temperature for sample 1, prepared without stabilizer at 40 °C.	37
Figure 4.13	The magnetization curve at room temperature for sample 2, prepared without stabilizer at 90 °C.	38
Figure 4.14	The magnetization curve at room temperature for sample 3, prepared with PVP stabilizer at 40 °C.	39
Figure 4.15	The magnetization curve at room temperature for sample 4, prepared with PVP stabilizer at 90 °C.	39
Figure 4.16	The magnetization curve at room temperature for sample 5, prepared with TOAB stabilizer at 90 °C.	40
Figure 4.17	Superparamagnetic component of sample 3.	40

Figure 4.18	Superparamagnetic component of sample 4.	41
Figure 4.19	Superparamagnetic component of sample 5.	41

Synthesis of Nano-Sized Cobalt oxide Nano-Particles Stabilized in Surfactant and Polymer Matrix and their Magnetic Properties

By

Fadi Mohammad Mostafa Naalweh

Supervisor

Dr. Sharif Musameh

Co-Supervisor

Dr. Mohammed Suleiman

Abstract

In this work, different-sized cobalt oxide nano-rods were selectively synthesized with narrow size distribution, by using chemical preparation methods, which could be carried out by the salt reduction technique. The samples were prepared at different temperatures, and two different types of stabilizer PVP and TOAB were added.

Smaller sizes of the samples were obtained in the presence of stabilizer, and the type of stabilizer had no effect on the size.

The size of the samples increased with increasing the temperature at which the synthesis of the nanoparticles was performed.

The magnetic measurements showed that the nano-rods had a superparamagnetic and paramagnetic character, which depended on the size of the samples and on the existence of the stabilizer. The type of stabilizer had affected the magnetic property of the samples. The superparamagnetic component of the sample that was prepared with Polyvinylpyrrolidone (*PVP*) stabilizer was stronger than that prepared with Tetraoctylammonium bromide (*TOAB*) stabilizer.

Chapter 1

Introduction

Chapter 1

Introduction

Nanoscience is one of the most important research and development activities in the border of modern science. The use of nanoparticle materials provides many unique advantages. Due to large volume-surface ratio, nano-sized materials show different physical and chemical properties in comparison to bulk materials (Faraji *et al.*, 2010).

The diameter of nanoparticles range from 1 to 100 nm in accordance with the term, made of inorganic material or organic, which have many novel properties compared with bulk materials (Wei *et al.*, 2008).

Due to the widespread applications of magnetic nanoparticles in different technological and biotechnological aspects, the preparation of different kinds of magnetic nanoparticles became very important nowadays (Faraji *et al.*, 2010).

Nanoparticles with various compositions are prepared by physical and chemical methods. The physical methods include evaporation, sputtering, laser ablation, ion ejection, and electron- beam lithography (Min *et al.*, 2009). The chemical methods include a salt reduction method, reverse micelles, electrochemical method, Sol-gel method, gas-liquid interface, thermolysis, and decomposition on ultrasonic treatment (Gubin *et al.*, 2005).

Magnetic nanoparticles are of great interest for scientists from a wide range of disciplines, as well as magnetic storage media, magnetic fluids, contrast

agents for magnetic resonance imaging (MRI), biolabelling and separation of biomolecules and magnetic targeted drug delivery (Wei *et al.*,2008).

The magnetic properties of nanoparticles appear as perfect when the size of the particles is decreased. Magnetic properties of nanoparticles differ significantly from its bulk counterpart. When the particle size is reduced below the single domain limit, they show a number of novel properties (Poddar *et al.*,2004).

One of the important characteristics of a magnetization is the coercive force (Gubin *et al.*, 2005). The amount of intensities of the magnetic field needed to reduce it to zero is called the coercivity. Decreasing the grain size of nanoparticles increases the coercivity (Tahir, 2008). Materials with low coercivity are called soft magnets; they can be used as cores for electro-magnets, electric motors, transformers, generators, and other electrical equipment. On the other hands, materials with high coercivity are called hard magnets; they may be used as fractional horse-power motors, automobiles, audio- and video- recorders, earphones, computer peripherals, and clocks (Dobrzański *et al.*, 2006).

Magnetic nanoparticles properties changes if the nanoparticles naturally oxidization or agglomeration with time. To protect the nanoparticles from these undesired processes, the nanoparticles can be coated using carbon, silica, precious metals, metal oxides, or stabilized in polymers and surfactants matrix (Faraji *et al.*, 2010).

1.1. Literature Review

There is a lot of work on the preparation of nanoscale samples in different ways and there are studies on the diagnosis and the properties of these samples; one of these properties is the magnetic property.

Karimian and his group prepared manganese oxide nanorod and cobalt oxide nanotube by a sol-gel reaction in reverse micelles. They studied the structure, the surface morphology of the manganese oxide nanorod by means of X-ray diffraction analysis, scanning electron microscopy, and transmission microscopy (Karimian *et al.*, 2012).

Magnetic $Zn_{1-x}Co_xO$ nanorods were fabricated via direct hydrothermal synthesis by Yang and his group. They showed that the nanorods had a ferromagnetic character and they were obtained with 98 and 36 Oe coercive fields H_c for nominal $x=0.029$ and 0.056 , respectively (Yang *et al.*, 2006).

A cobalt nanoplatelet samples were synthesized with different hcp phase contents by a novel reduction process. Jiangong and his group found that the saturation magnetization of the nanoplatelet powders was lower than the corresponding bulk value and the coercivities of the nanoplatelets increased with the hcp phase content (Jiangong *et al.*, 2004).

Pamela and his group, Prepared Co nano powders of 30 - 70 nm. They studied the characterization using XRD, SEM, TEM and VSM. The results of VSM showed a higher saturation magnetization at 100 K of the nano cobalt compared with that for the bulk metal (Pamela *et al.*, 2011).

Nickel (Ni) electrodeposited inside Cobalt (Co) nanotubes was fabricated by Narayanan and his group, using a two-step potentiostatic electro

deposition method with an average diameter of 150 nm and length of ~15 μm . They found that the Ni and Co nanorods exhibited a very high longitudinal coercivity (Narayanan *et al.*, 2010).

A metallic Co nanorods (about 100 nm in diameter) formed inside an array of anodized aluminum oxide AAO nanopores synthesized by Aslam and his group. They found that the increase of nanorod length led to increase the coercivity and thermal activation volume (Aslam *et al.*, 2005).

Shihua and his group, prepared Co nanoparticles by metal vapor synthesis technique. They studied the characterization and properties by TEM, XRD, temperature-programmed desorption, chemisorption, magnetic measurements. They concluded that the particle size of Co powder depends on the initial Co concentration in the toluene matrix, and the Co powder indicates ferromagnetic behavior (Shihua *et al.*, 2003).

Cobalt nanoparticles by hydrothermal method were synthesized by Pauline and his group. The particle size decreased as the annealing temperature increases (Pauline *et al.*, 2012).

Jianchun and his group, fabricated nanotubes and nanowires cobalt in the same alumina template modified with an organ amine, which was an important factor to control nanostructure shapes. They indicate that the shape anisotropy had an effect on the magnetic properties (Jianchun *et al.*, 2004).

Mixture of crystalline $\text{Co}_3\text{O}_4/\text{CoO}$ nanorods with an average length of around 80 nm and an average diameter of 42 nm by microwave hydrothermal technique were synthesized by Al-Tuwirqi and his group.

They characterized it by XRD, FE-SEM, energy-dispersive, EDX, and FT-IR methods (Al-Tuwirqi *et al.*, 2011). They found that the magnetic hysteresis loops at room temperature have soft magnetic behavior.

Yue and his group, synthesized single-phase CoFe_2O_4 nano-particles by the Co-precipitation method by adding the mixed solutions of Co^{+2} and Fe^{+3} ions into the NaOH solutions (Yue *et al.*, 2010). They pointed out that the increase in concentrations of the NaOH solutions increased the crystallite sizes and the existence of the outer layers made decreased in M_s and increased in H_c .

1.2. Objectives

In this work, different cobalt oxide nanorods selectively are synthesized with narrow size distribution. The magnetic properties of these nanorods as a function of size at different temperatures are studied.

This can be summarized as follows:

- Synthesis of nano-sized Cobalt oxide nanorods stabilized in surfactant and in polymer matrix.
- Studying the effect of the stabilizing matrixes on the size and the structural properties of the nano-sized Cobalt oxide particles.
- Finding out the magnetic types of these particles. And studying the effect of the size and the stabilizing matrixes on the magnetic property.

The nanorods preparation is performed by using salt reduction method. The advantages of these preparation methods are simple and cheap. In addition, large amounts of nanorods can be prepared without impurities.

Moreover, the size of the magnetic nanorods can be controlled easily by varying the preparation parameters, such as the temperature, the solvent.

To prevent undesired aggregation and agglomeration the nanorods is stabilized in a matrix. Two different stabilizing matrixes are used: polymer and surfactant matrix. The effect of the stabilizing matrixes on the size and the properties of these nanoparticles is also studied.

This thesis is organized as follows. Chapter Two presents a theoretical background of magnetism. Chapter Three addresses the devices used in the study as well as the tools and the methods used in the preparation of the samples. Chapter Four introduces the results of the present work as well as a summary of conclusions and suggestions for future work.

Chapter 2

Theoretical Background

Chapter 2

Theoretical Background

2.1. Magnetization (\mathbf{M}):

The Magnetization \mathbf{M} is defined as the total magnetic dipole moments (\mathbf{m}) induced per unit volume (V) of the material. Therefore, \mathbf{M} can be written as

$$\mathbf{M} = \mathbf{m}/V \quad (1)$$

Mass magnetization (\mathbf{M}_g), however, is the total magnetic dipole moments per unit mass (g) of the material. Thus \mathbf{M}_g is given by

$$\mathbf{M}_g = \mathbf{m}/g \quad (2)$$

Where the cgs unit of \mathbf{M}_g is emu/g.

Magnetic materials acquire a magnetic dipole moment when the material is magnetized if it is placed in a magnetic field. The magnetic dipole moments of the elementary current loop in the material become aligned parallel to the field (Bandoyopadhyay, 2008).

2.3. Relation between \mathbf{B} , \mathbf{H} , and \mathbf{M} :

For most substances, magnetic flux \mathbf{B} saturates at high applied magnetic field \mathbf{H} , but in some materials, \mathbf{B} is a linear function of \mathbf{H} .

The equation relating \mathbf{B} , \mathbf{H} , and \mathbf{M} (in cgs units) is given by (Denny *et al.*, 2010).

$$\mathbf{B} = \mathbf{H} + 4\pi\mathbf{M} \quad (3)$$

2.4. Magnetic Susceptibility χ_m :

The magnetization \mathbf{M} is proportional to the applied field of isotropic linear materials (Denny *et al.*, 2010), so that:

$$\mathbf{M} = \chi_m \mathbf{H} \quad (4)$$

Where χ_m is the magnetic susceptibility of that material, which is defined as the intensity of magnetization gained from the material for unit field strength (Murugesan, 2008). Hence,

$$\chi_m = \frac{M}{H} \quad (5)$$

So the relation between \mathbf{B} and \mathbf{H} , (in cgs units) for isotropic linear material can be written as:

$$\mathbf{B} = (1 + 4\pi\chi_m) \mathbf{H} = \mu\mathbf{H} \quad (6)$$

Where μ is the permeability of the isotropic linear material, which is given by

$$\mu = 1 + 4\pi\chi_m \quad (7)$$

Magnetic materials can be classified according to the susceptibility χ_m (or permeability μ). If χ_m is negative (i.e., $\mu < 1$), the material is called diamagnetic. If χ_m is positive (i.e., $\mu > 1$), the material is paramagnetic, while if χ_m is positive and very large (i.e., $\mu \gg 1$), the materials are ferromagnetic.

Figure 2.1 shows alignments of a magnetic dipole moment at room temperature in zero applied-field for different types of magnetic materials.

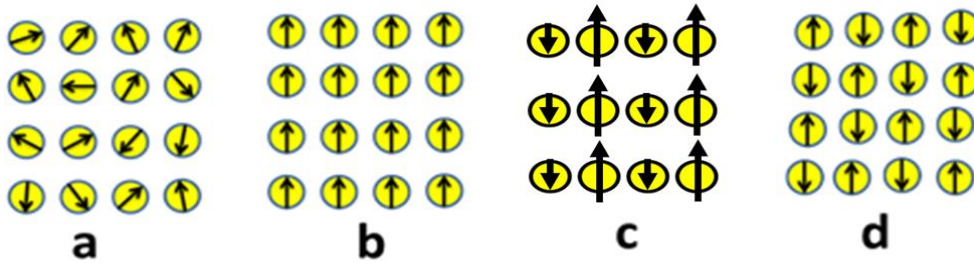


Figure 2.1: alignments of magnetic dipole moment at room temperature in zero applied-field. (a) paramagnetic material, (b) ferromagnetic material, (c) ferrimagnetic material, and (d) anti ferromagnetic material.

The magnetic susceptibility of ferromagnetic materials will be different and it depends on the temperature according to the equation:

$$\chi_m = \frac{C}{T \pm \theta} \quad (8)$$

Where C is the Curie constant, T is the room temperature, and θ the critical temperature, T and θ are in Kelvin unit. For diamagnetic material, χ_m does not depend on the temperature as shown on figure 2.2, while for paramagnetic material $\chi_m = C/T$. The critical temperature for ferromagnetic and ferrimagnetic material called Curie temperature (T_c). For antiferromagnetic material the critical temperature is called Neel Temperature (T_N) (Mathias, 2008).

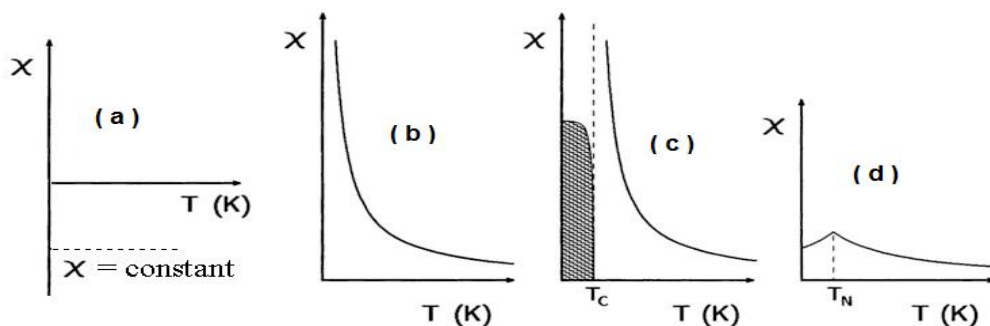


Figure 2.2: Temperature dependence of the magnetic susceptibility of (a) diamagnetic, (b) paramagnetic, (c) ferromagnetic and ferrimagnetic, and (d) antiferromagnetic materials.

In the presence of a uniform magnetic field there are different interactions taking place such as the attractive forces which arise mainly from electrostatic.

For small spherical particles at small separation, the attraction energy was derived by Hamaker and is given by (Chikazumi, 1964):

$$U = - AD/24 S \quad (9)$$

$$\text{For } D \gg S > 4A$$

Where D is the particle diameter, S is surface separation of the particles, $A = \pi^2 n \lambda$, n is the number of atoms/cc (where cc is centimeter cubic), and $\lambda = 3/4 (h\nu_0 \alpha^2)$, where α is the polarizability of the material and $h\nu_0$ is the ionization energy.

For $S \gg D$, the attraction energy is given by:

$$U = -16 A/9 (D/2 S)^6 \quad (10)$$

Where the $S = X - D$, where X is the center to center separation.

The other attractive forces are the magneto static (dipole – dipole interaction). The energy of this interaction depends on the magnetic moment of these dipoles and the maximum energy is given by (Chikazumi, 1964)

$$U_{\max} = - \pi^2 D^3 M_s^2/18 \quad (11)$$

When the dipoles are parallel and the magnetic moments of the dipoles are equal.

The other forces are the repulsive which are due to thermal agitation and also arise from the coating of the particles. This energy is given by $k_B T$.

In zero field, the magnetic structure of ferromagnetic materials consists of the region (domains) whose magnetization vectors are oriented so as to minimize the magneto static energy of the material. Each domain consists of ferromagnetically aligned moments. There is a gradual rotation of spin directions between neighboring domains (known as the Bloch wall), which occurs over a distance of several hundred Angstroms (Cullity , 1972, Chikazumi, 1964).

A single domain particle is one which its diameter below a critical size and that particle in a state of uniform magnetization at any field (Bean *et al.*, 1959, Nee'l, 1949).

2.5. Diamagnetism:

Diamagnetism is defined as a very weak form of induced or temporary magnetism for which the magnetic susceptibility is negative and temperature independent.

The magnetization of the diamagnetic material is very small and in the opposite direction of the applied magnetic field direction (Robert *et al.*, 2004).

Diamagnetic materials have no angular momenta and without compensating spin (Roman, 1999), but magnetic dipoles are induced by the external field (figure 2.3). It is induced due to an applied magnetic field by a change in the orbital motion of electrons, which is according to the

Lenz's law, are aligned opposite to the applied field direction, (Wolfgang *et al.*, 2009, William *et al.*, 2001).

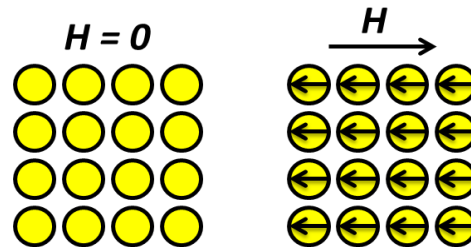


Figure 2.3: The atomic dipole configuration with and without a magnetic field in a diamagnetic material.

Almost all the organic substances, metals like Bismuth (Bi), Zinc (Zn) and Mercury (Hg), nonmetals like Sulfur (S), Jodium (J) and Silicon (Si), and superconductors below the critical temperature are the kinds of diamagnetic materials (Wolfgang *et al.*, 2009).

2.6. Paramagnetism:

Paramagnetism is a relatively weak form of magnetism that is produced from the independent alignment of magnetic dipoles with an applied magnetic field (William *et al.*, 2001). The magnetization is small and oriented parallel to the applied magnetic field (Robert *et al.*, 2004).

Curie was the first who had taken a measurement of magnetic susceptibility in paramagnetic material, and he found that it depends on the temperature (Denny *et al.*, 2010).

2.7. Ferromagnetism:

The ferromagnetism is defined as positive spin interactions when the spins are all aligned in the same direction, which results from the parallel alignment of neighboring magnetic moments (Bandoyopadhyay, 2008). It

exists in some materials like Iron (Fe), Cobalt (Co), and Nickel (Ni) which are naturally magnetically ordered and which develop unprompted magnetization without the need for an applied magnetic field (Robert *et al.*, 2004).

Magnetizations in Ferromagnetism are very strong and permanent (William *et al.*, 2001). At temperatures below the Curie temperature, the magnetic moments within domains of ferromagnetic materials are aligned parallel, above the Curie temperature ferromagnetic materials turn into paramagnetic behavior. For example, the Curie temperature of Fe is 770 °C, that of Ni is 358 °C and that of Co is 1131 °C (Denny *et al.*, 2010).

2.8. Antiferromagnetism:

A phenomenon detected in some materials; the nearest-neighbor moments in antiferromagnetic substances are aligned antiparallel, which causes complete magnetic moment cancellation (William *et al.*, 2001).

The theory of antiferromagnetism was developed by Neel (Nee'l, 1949). The magnetic susceptibility of antiferromagnetic material increases as temperature increases until it reaches Neel's temperature where antiferromagnetism takes paramagnetic behavior (Roman, 1999).

The Neel temperatures for some antiferromagnetic materials are for Iron Oxide (FeO) 198 K, Nickel fluoride (NiF₂) 73.2 K and Cobalt Oxide (CoO) 328 K. The permeability of antiferromagnetic materials is larger than unity (Walter *et al.*, 2002).

2.9. Ferrimagnetism:

Ferrimagnetism is found in some ceramic substances. The magnetization is permanent and large. It is produced from incomplete magnetic moment cancellation and antiparallel spin coupling, (William *et al.*, 2001).

Ferrimagnet, as ferromagnet has spontaneous magnetization below a critical temperature, but for high temperatures, the material changes to a paramagnetic behavior (Wolfgang *et al.*, 2009).

The magnetic moments in ferrimagnetic materials are arranged in a similar way to antiferromagnetic materials, and if the magnetic moment in one direction much more than another direction, the output magnetic moment is non-zero (Bandoyopadhyay, 2008).

2.10. Superparamagnetism:

Superparamagnetism is one of the magnetism kinds; superparamagnetic substances consist of a small ferromagnetic cluster (Shah, 2010).

A small ferromagnetic nanoparticle consists of a single domain. Internal forces and external magnetic field H determine the direction of its magnetization M . There is no hysteresis for superparamagnetic materials (Mathias, 2008).

The magnetic moment carriers of this material are particles ($\mu \approx 10^4 \mu_B$), which are composed of $\approx 10^4$ atoms, where μ_B is the Bohr magneton. The superparamagnetic materials invariably (constantly) contain a particle size distribution. The behavior of a superparamagnetic material is often described by a modified Langevin function.

The particle size distribution is required to explain the magnetic properties of the superparamagnetic system. For particles with spherical shape, the total magnetization can be evaluated by considering the Langevin function with a log – normal distribution (Cullity , 1972):

$$M/M_s = \int L(y) f(y) dy \quad (12)$$

Where $L(y)$ is the Langevin function, M is the total magnetization of the sample, M_s is the saturation magnetization, $f(y)$ is a log – normal distribution function with a median diameter value D_v and a standard deviation and $y = D/D_v$, where D is the diameter of the particle.

The magnetic properties of superparamagnetic materials are governed by the relative properties of the three energies:

- The anisotropic energy of particles.
- The Zeeman energy, which is due to the coupling between the magnetic field (local and applied) and the moment of the particles.
- The thermal energy, which tends to change the orientation of the magnetic moment in the individual particle.

The ratios of these three energies determine which type of magnetic relaxation mechanism occurs.

The magnetic relaxation can take place by two distinct mechanisms:

The Neel relaxation in which, the direction of the moment of the particle is changed out of the easy direction against the magnetic anisotropy of the particle.

The relaxation time τ_N for this process is given by Nee'l (Nee'l, 1949)

$$\tau_N = \tau_o \exp(x) x^{-1/2} \quad \text{for } x > 2 \quad (13)$$

Where $x = KV'/K_B T$. Where V' is the magnetic volume of the particle, K_B is the Boltzmann constant, T is the thermal agitation, K is the anisotropy constant, $\tau_o = 10^{-11}$ s, and τ_N is the relaxation time in kelvin unit.

The other relaxation takes place through the rotation of the particle while the magnetic moment is held fixed by the magnetic anisotropy in the easy direction. This is known as Brownian relaxation and is given by (Nee'l, 1949):

$$\tau_B = 3 V \eta_o / k_B T \quad (14)$$

Where η_o is the viscosity of the carrier, and V is the hydrodynamic volume of the particle.

Chapter 3

Experimental Work

Chapter 3

Experimental Work

In this chapter, the devices used in the study will be described. The tools and the methods used in the preparation of the samples will be presented.

3.1 Experimental Equipment and tools:

3.1.1 FT-IR spectroscopy:

Fourier Transform Infra-Red spectroscopy FTIR (figure 3.1) was used by organic and inorganic chemists to find the composite material in the samples used.

An IR beam hits the sample, some of the IR radiation is transmitted through the sample and the other absorbed by the sample. Measurements of different IR frequencies give different peaks, which represent the sample compounds.



Figure 3.1: Fourier Transform Infra-Red spectroscopy.

The FTIR spectroscopy can be used to analyze solid, liquid and gas samples (Frank, 1997).

The general uses of the FTIR spectroscopy are for identifying unknown materials; organic and inorganic compounds, determining the quality or consistency of a sample, and the amount of components in a mixture (Frank, 1997).

3.1.2 Scanning Electron Microscopy (SEM):

SEM is a microscope that gives images of surface topography with high resolution. It has a magnification range of 5 to 300 000 times, and acceleration voltage parameter of 0.5 to 30.0 kV (Roa *et al.*, 2010). Surface characteristics (electrical conductivity, chemical composition.) are provided by this microscope (Paul *et al.*, 2012). The SEM that was used for the imaging of the samples is JEOL JSM-6060LV Low Vacuum Scanning Electron Microscope that was used is shown in figure 3.2.



Figure 3.2: Scanning Electron Microscopy (SEM).

3.1.3 Energy dispersive X-ray spectroscopy (EDS)

Energy dispersive X-ray spectroscopy (EDS) is an analytical technique which is used for the elemental analysis of nanoparticles and nanomaterial's. It is an integral part of scanning electron microscope (SEM) and transmission electron microscope (TEM) (Ming *et al.*, 2012).

EDS characterizes the elemental composition of a component by using X-ray emissions (Alberto *et al.*, 2008). A schematic of an EDS system is offered in figure (3.3).

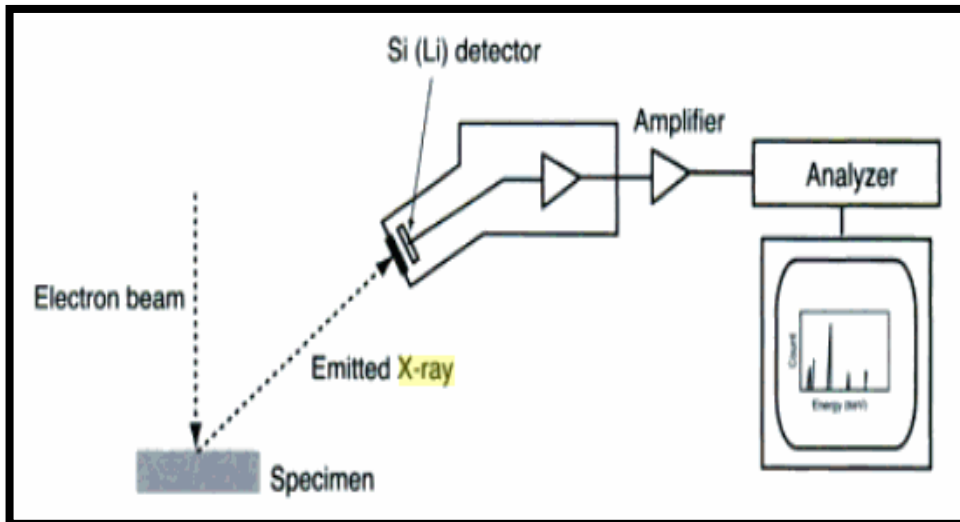


Figure 3.3: Schematic diagram of an energy dispersive X-ray spectroscopy system

3.1.4 Vibrating Sample Magnetometer (VSM)

The Model 3900 MicroMag™ high-performance vibrating sample magnetometer and high sensitivity is used for magnetic measurements to specify the kind of the nano-rods prepared in this work (figure 3.4). Magnetometer system is highly accurate 2% vs., Sensitive of 0.5 μemu standard deviation at room temperature (Princeton Measurements Corporation, 2009)].

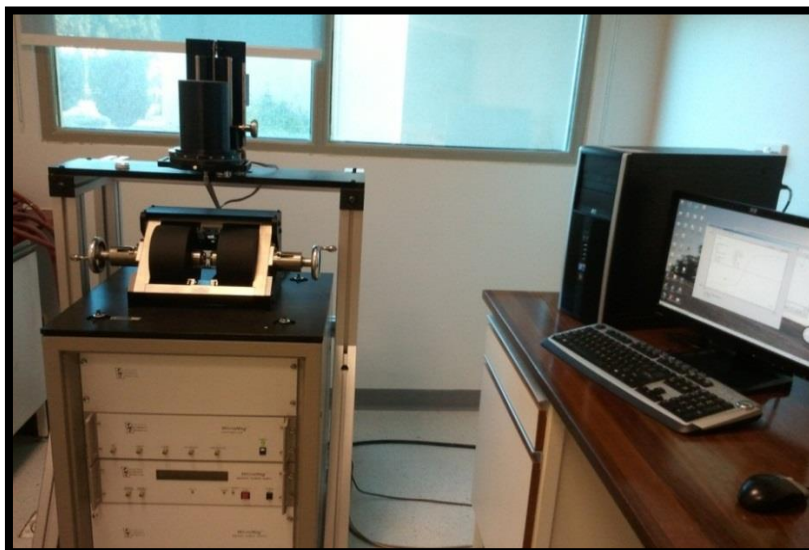


Figure 3.4: Vibrating Sample Magnetometer (VSM).

The principal work of Magnetometer is by vibrating the specimen vertically at the midpoint of the field.

Magnetic dipole moment versus applied field are obtained by using the VSM.

3.2 Chemicals and components:

All the chemicals were bought in dry pure form, and used without additional treatments. Cobalt (II) chloride hexahydrate ($CoCl_2 \cdot 6H_2O$) was purchased from Sigma-Aldrich Company. Sodium hydroxide ($NaOH$) was purchased from Frutrarom Company.

Polyvinylpyrrolidone (PVP) was purchased from Alzahra factory.

Tetraoctylammonium bromide ($TOAB$) was purchased from Sigma-Adriatic with 98% purity.

3.3 Sample preparation:

The samples were prepared by one of the chemical techniques called salt reduction method with different states. The first one was prepared without

adding any stabilizer, the second by using *PVP* stabilizer and the third by using *TOAB* stabilizer as:

3.3.1 Salt reduction method without any stabilizer:

An amount of 0.9g of $\text{CoCl}_2 \cdot 6\text{H}_2\text{O}$ was dissolved in 50ml of distilled H_2O . The solution was mixed and stirred at constant temperature (40°C , and 90°C) in shaking water bath; using a stirring rate of 120 rpm .

A 1.6g of NaOH was dissolved in 200ml of distilled H_2O and then added stepwise 150ml of the NaOH solution to the cobalt ion solution.

The preparation process lasted for two hours with the same temperature and stirring rate. The pH was greater than 9 throughout the reactions.

When the reaction was completed, precipitate was shown at the bottom of the reaction mixture, which was kept at least for 12 hours. The precipitate separated from the solution, and it was washed for several times with distilled H_2O , then the precipitate was dried at 80°C .

The procedure that was used, is summarized in figure 3.5.

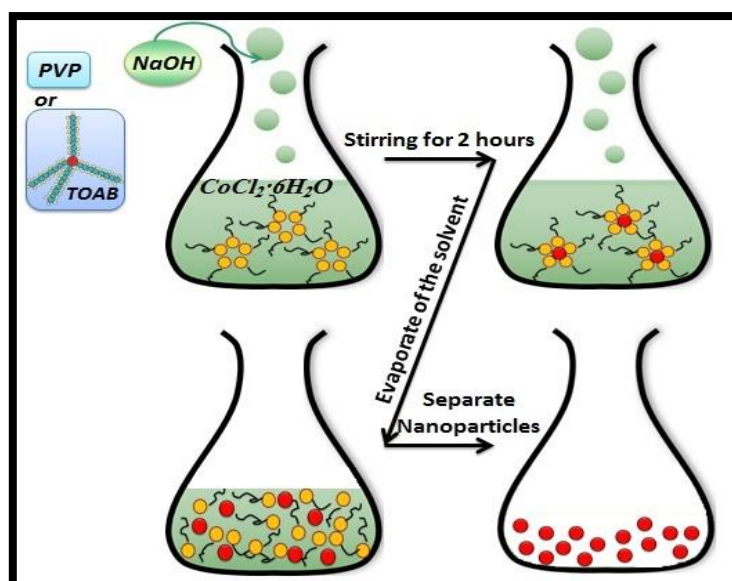


Figure 3.5: Schematic of preparing samples by the salt reduction method.

3.3.2 Salt reduction method in the presence of *PVP* stabilizer:

In this method, 0.5g of Polyvinylpyrrolidone (*PVP*) surfactant was dissolved in 50ml distilled H₂O.

PVP solution with the cobalt ion solution at the constant temperatures (40 °C, and 90 °C) was placed in a shaking water bath and a stirring rate of 120 rpm.

3.3.3 Salt reduction method in the presence of *TOAB* stabilizer:

An amount of 0.5g of Tetraoctylammonium (*TOAB*) surfactant was dissolved in 50ml distilled H₂O.

TOAB solution was mixed with the cobalt ion's solution at constant temperatures (90 °C) in a shaking water bath using a stirring rate of 120 rpm.

Chapter 4

Results and Discussion

Chapter 4

Results and Discussion

4.1 Sample Characterization:

The cobalt oxide samples were prepared under different conditions. Some of the samples did not contain any stabilizer and the others contained two different types of the stabilizer. Besides, the preparation was done at different temperatures as shown in the following table (Table 4.1).

Table 4.1 The samples with the conditions in which they were prepared

Sample No. For Cobalt Oxide	Temp. Preparation	Stabilizer
1	40 °C	Without stabilizer
2	90 °C	
3	40 °C	Polymer stabilizer (PVP)
4	90 °C	
5	90 °C	Surfactant stabilizer (TOAB)

4.1.1 FT-IR Spectroscopy:

The FT-IR spectra of transmittance versus wavenumber for sample 1 and 2 that are prepared without any stabilizer at 40°C and 90 °C of temperature at which the preparation was performed are presented in figures 4.1 and 4.2. The results show that there is a characteristic peak at the positions 621-715 cm⁻¹, and 2340-2360 cm⁻¹, which could be assigned to Co-O cobalt oxide

peak, and carbon dioxide CO_2 , respectively, by comparing these results with standard.

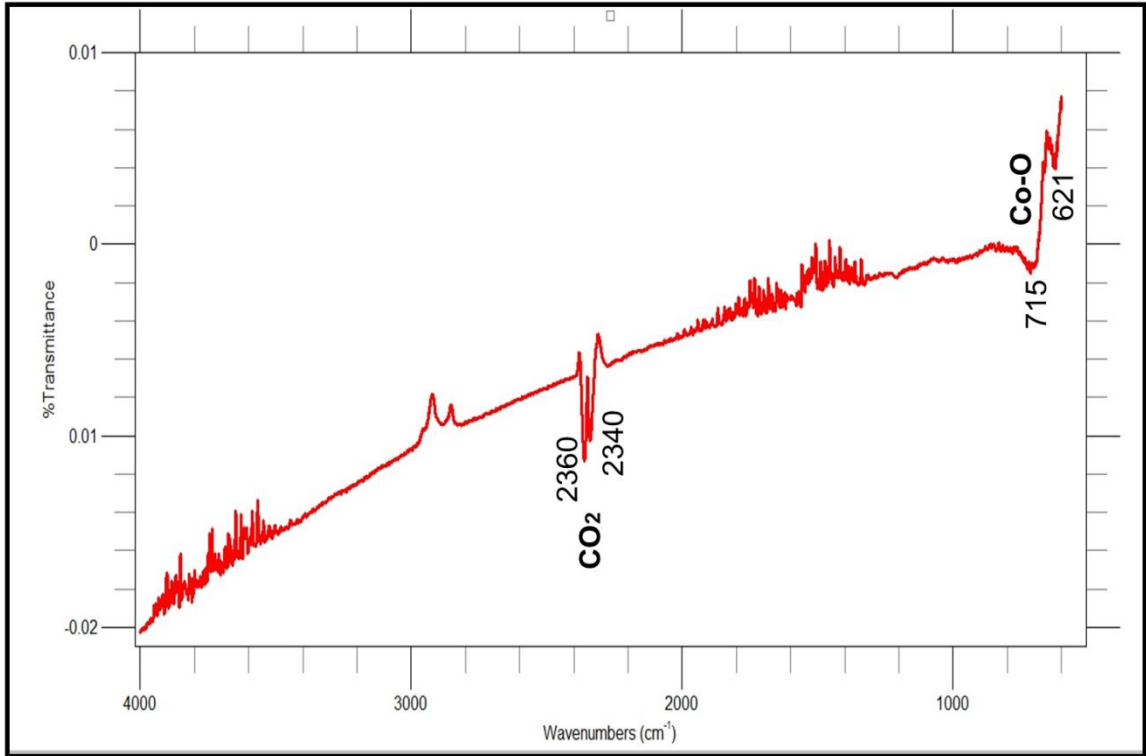


Figure 4.1: FT-IR spectrum of transmittance versus wavenumber for sample 1.

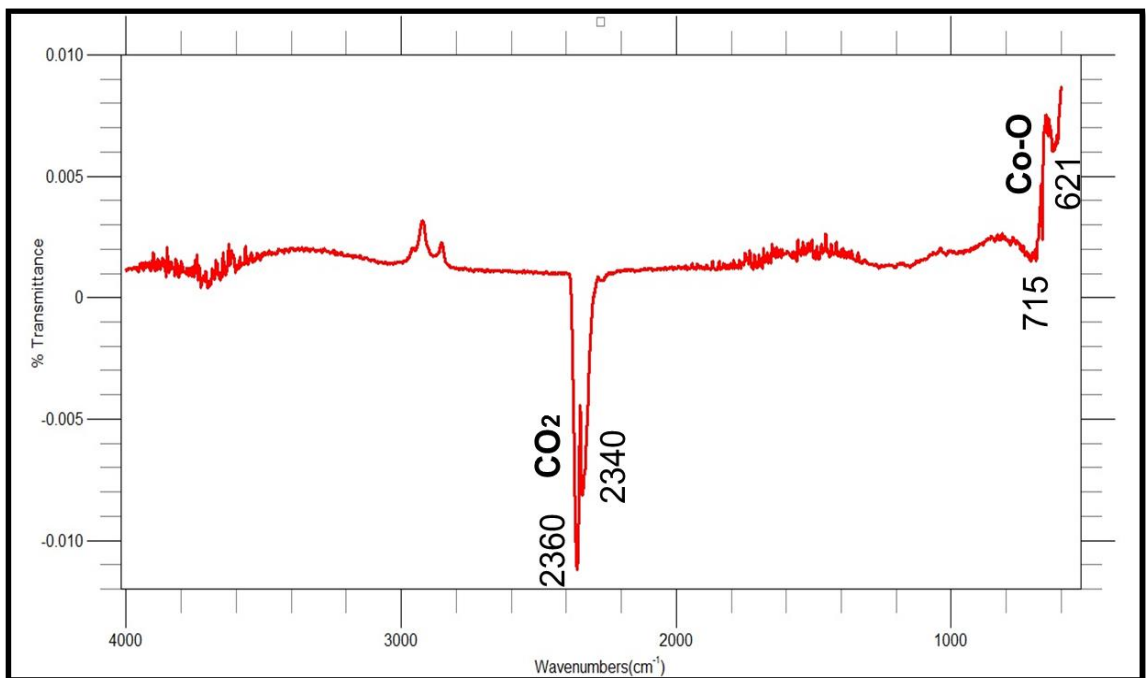


Figure 4.2: FT-IR spectrum of transmittance versus wavenumber for sample 2.

FT-IR spectra of samples that is prepared with PVP stabilizer at 40 °C and 90 °C of temperature at which the preparation was performed for sample 3 and 4, respectively, are presented in Figs 4.3 and 4.4. For sample 5 that is prepared with TOAB stabilizer at 90 °C of temperature at which the preparation was performed, FT-IR spectra is presented on figure 4.5.

The FT-IR spectra of all samples show a characteristic absorption in the range 502-746 cm^{-1} which represented to Co-O cobalt oxide peak and it is in a good agreement with literature (Chih *et al.*, 2004).

The FT-IR spectra for all stabilized samples show a characteristic peak at the positions 1450 cm^{-1} , 1492 cm^{-1} , 1600 cm^{-1} , and 2922-3024 cm^{-1} for samples 3, 4 and 5, which could be assigned respectively, to C-C bond, C-H bond, C-N stretching, and C-H stretching.

These characteristic peaks did not appear in the non-stabilized sample. These results show that the nanoparticles are stabilized by the matrix which was used for stabilizer (PVP and TOAB).

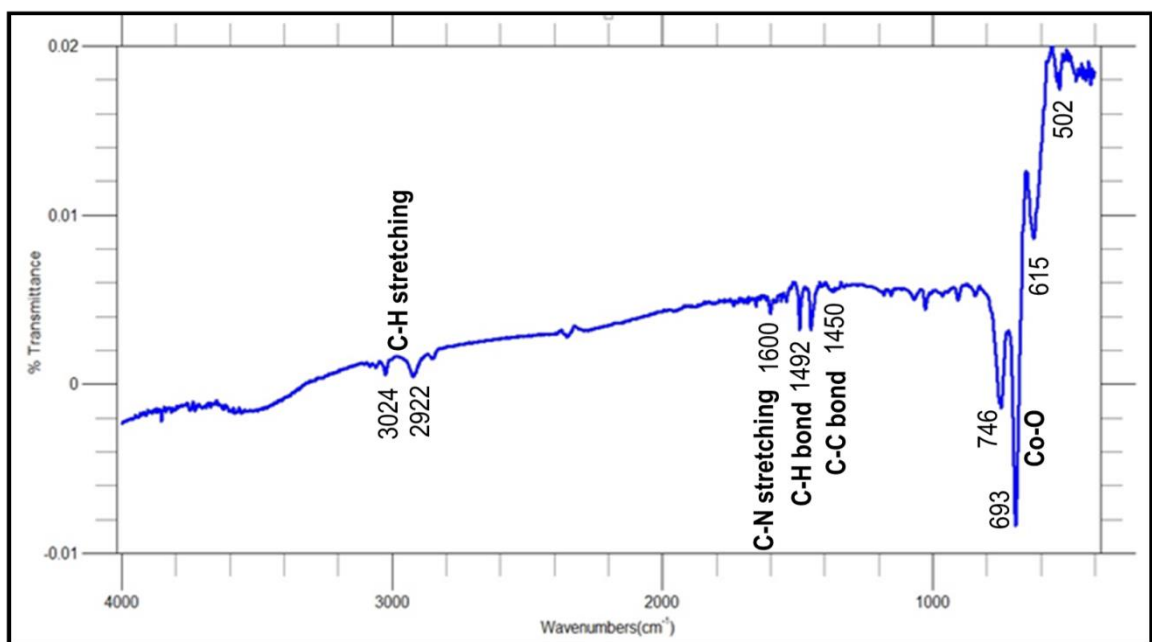


Figure 4.3: FT-IR spectrum of transmittance versus wavenumber for sample 3.

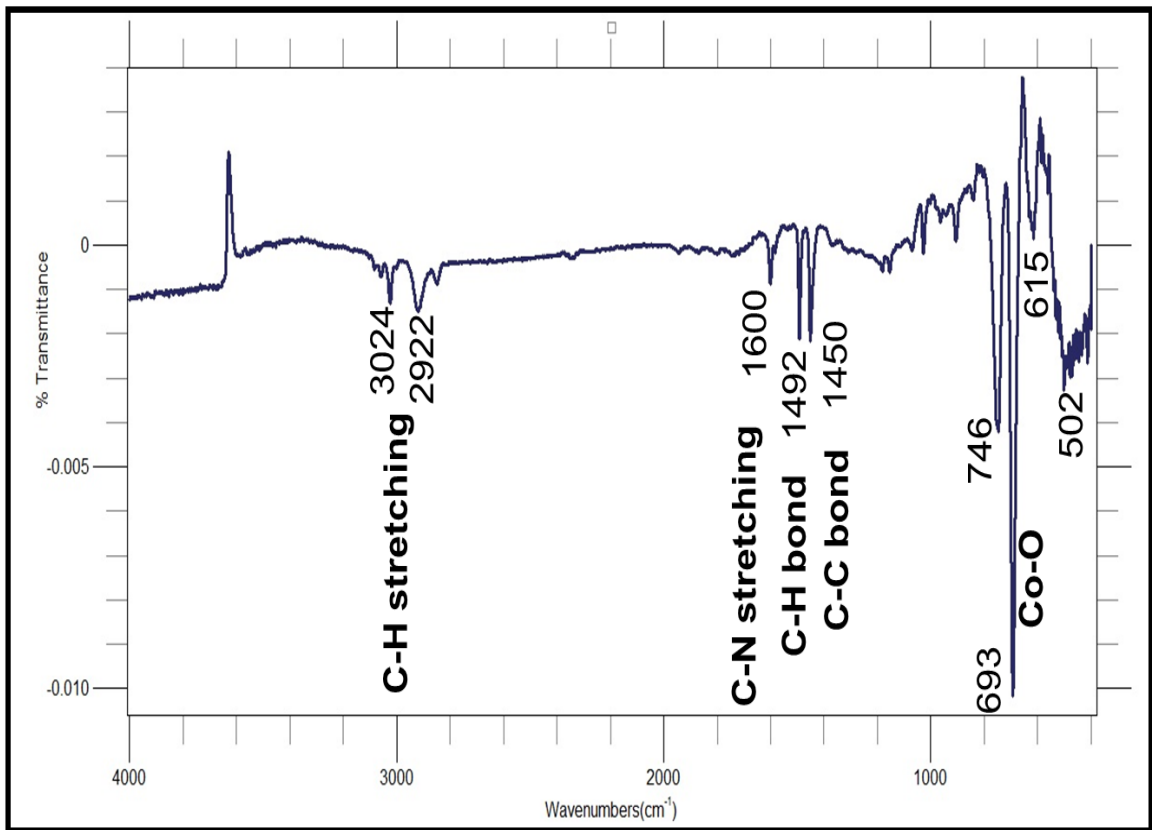


Figure 4.4: FT-IR spectrum of transmittance versus wavenumber for sample 4.

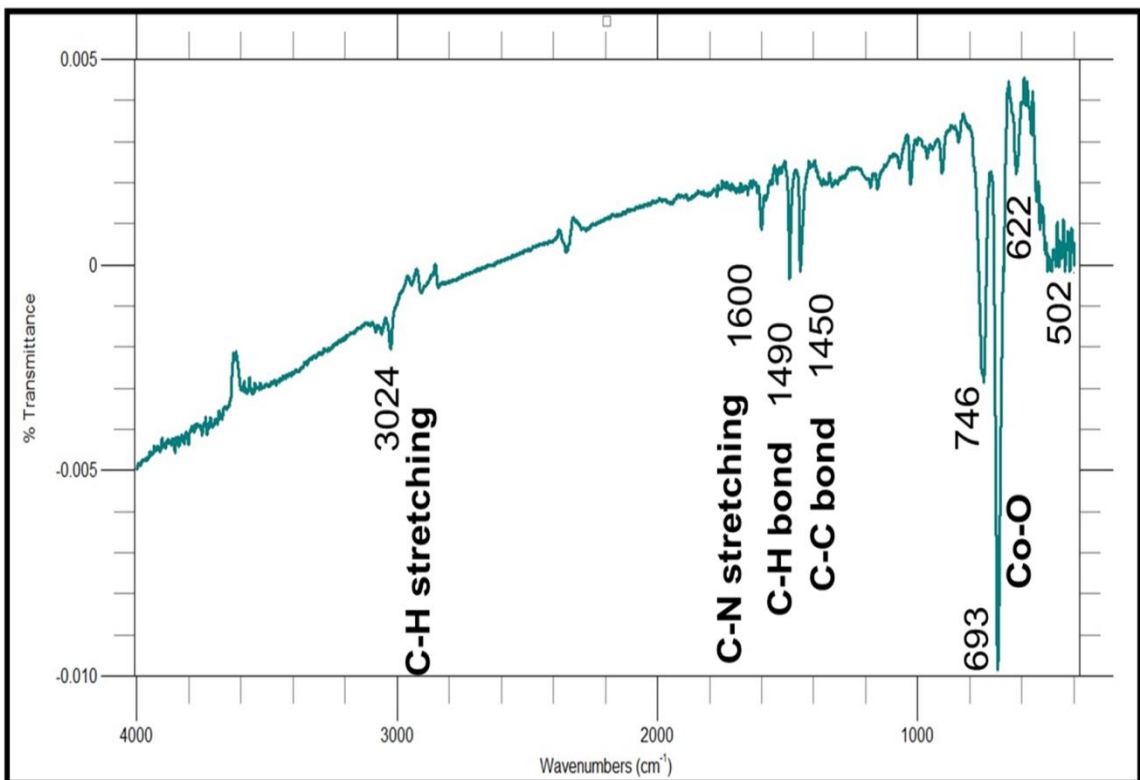


Figure 4.5: FT-IR spectrum of transmittance versus wavenumber for sample 5.

4.1.2 Energy Dispersive X-ray Spectroscopy (EDS) Measurements:

EDS measurements were used to identify and differentiate the chemical composition of the desired sample. Sample 2 was subjected to EDS measurement that has signs belonging to its composition, represented in figure 4.6. The results contained signs of carbon at 0.2 keV, oxygen signs at 0.6 keV, Co-L signs at 0.8 keV, and Co-K signs at 6.9 keV.

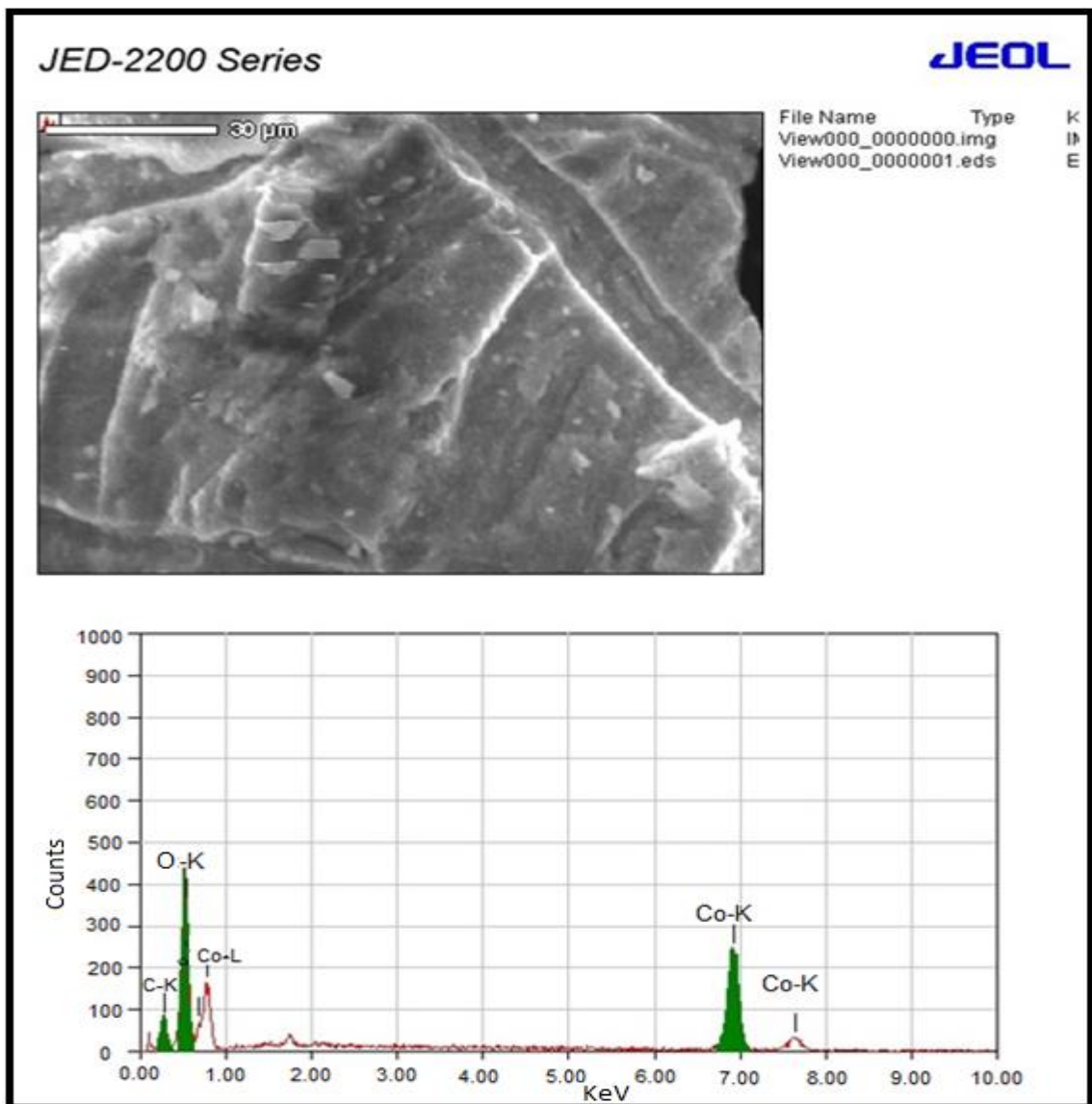


Figure 4.6: EDS measurement for sample 2.

Comparing the EDS results with the FT-IR results there is a good evidence that no chloride still coordinating the Co. This is an evidence that cobalt chloride is completely oxidized into Co-O form, indicating the formation of nano-metallic particles from the starting metal salt.

4.1.3 Scanning Electron Microscopy Measurements

SEM measurements for samples that were prepared without any stabilizer at 40 °C and 90 °C temperature at which the synthesis was performed are shown in figures 4.7 and 4.8. They show that the size is in the micrometer scale with length about 260 μm , and width 120 μm for sample 1, and 390 μm of length and 230 μm width for sample 2.

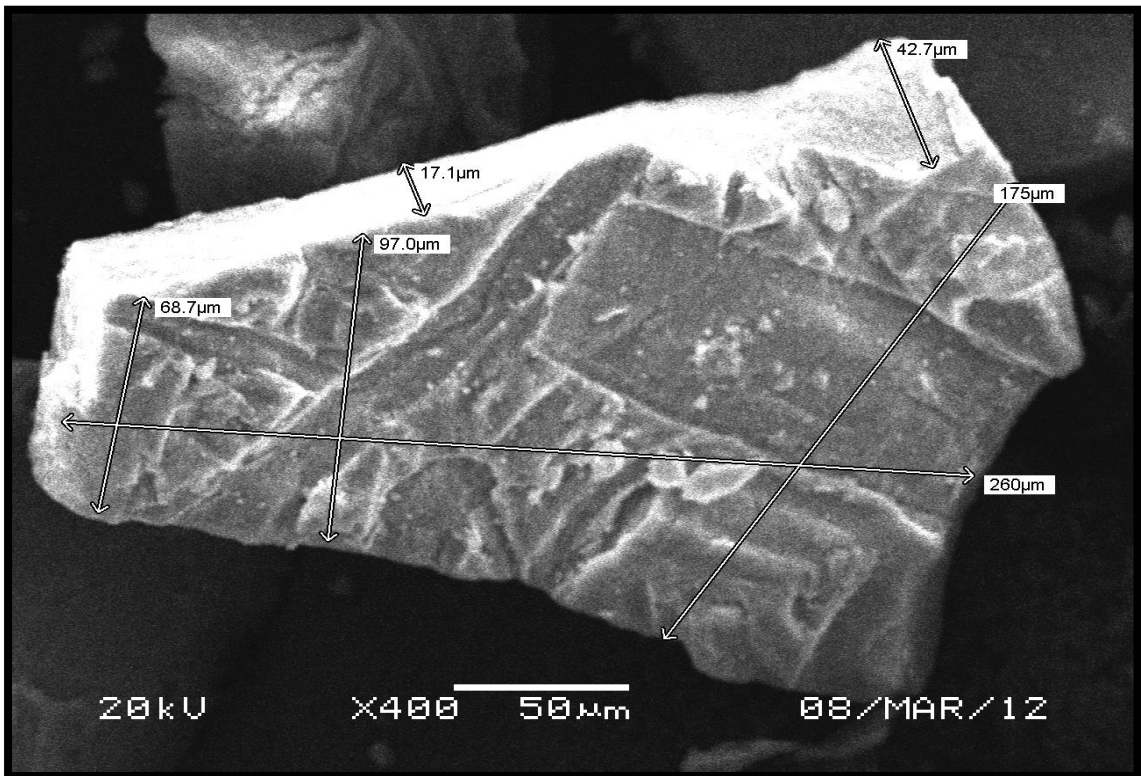


Figure 4.7: SEM for Sample 1.

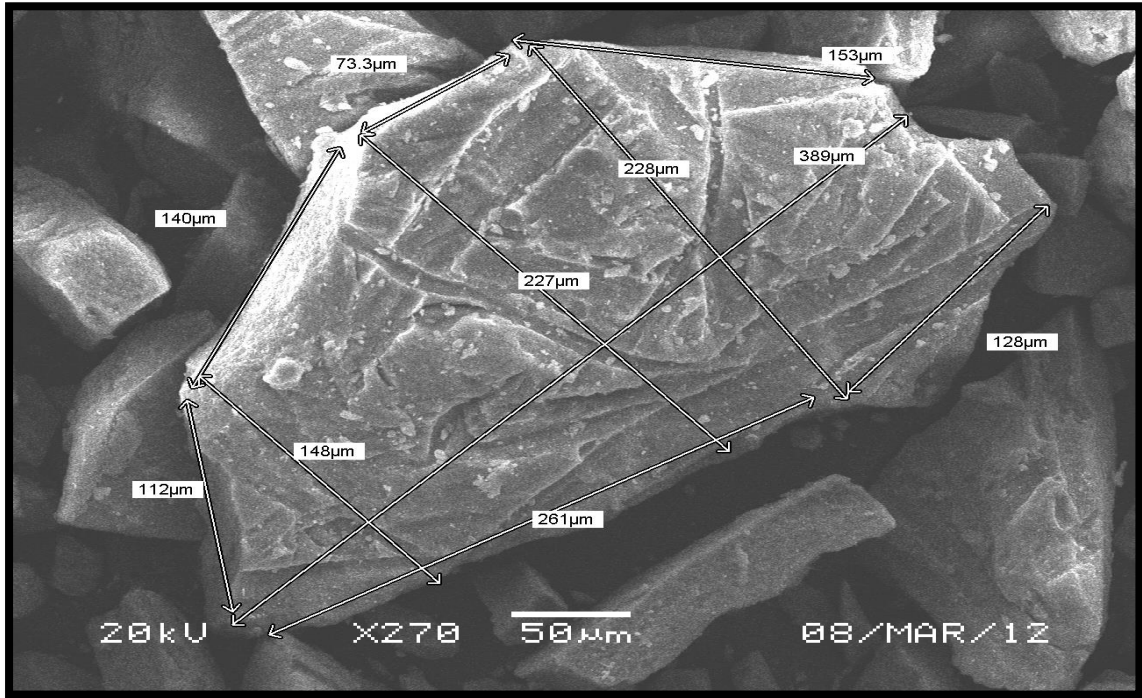


Figure 4.8: SEM for Sample 2.

The SEM measurements for samples that were prepared with PVP stabilizer at 40 °C and 90 °C temperature, at which the synthesis was performed, are shown in Figs. 4.9 and 4.10 for sample 3 and 4, respectively. It appears that the samples are nanorods with length in the range 150-170 nm for sample 3 and 160-250 nm for sample 4. The width for samples 3 and 4 is in the range 40-50 nm.

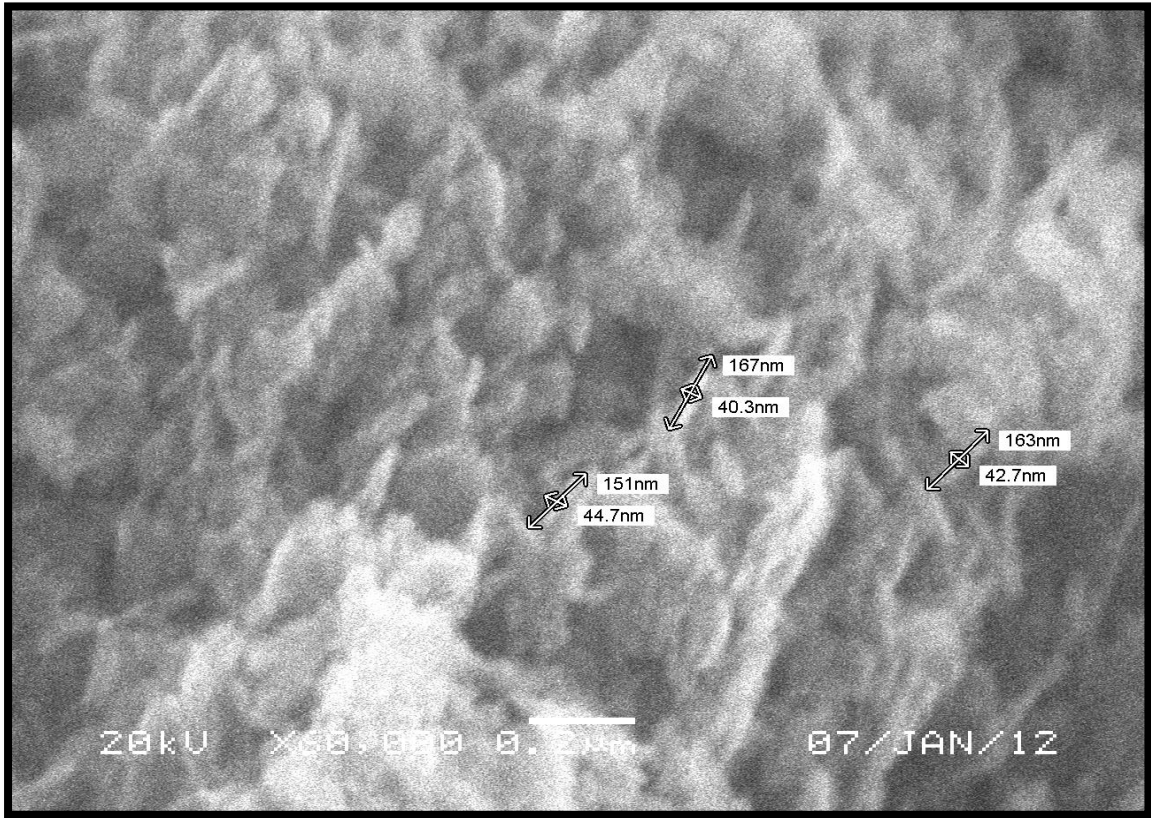


Figure 4.9: SEM for Sample 3.

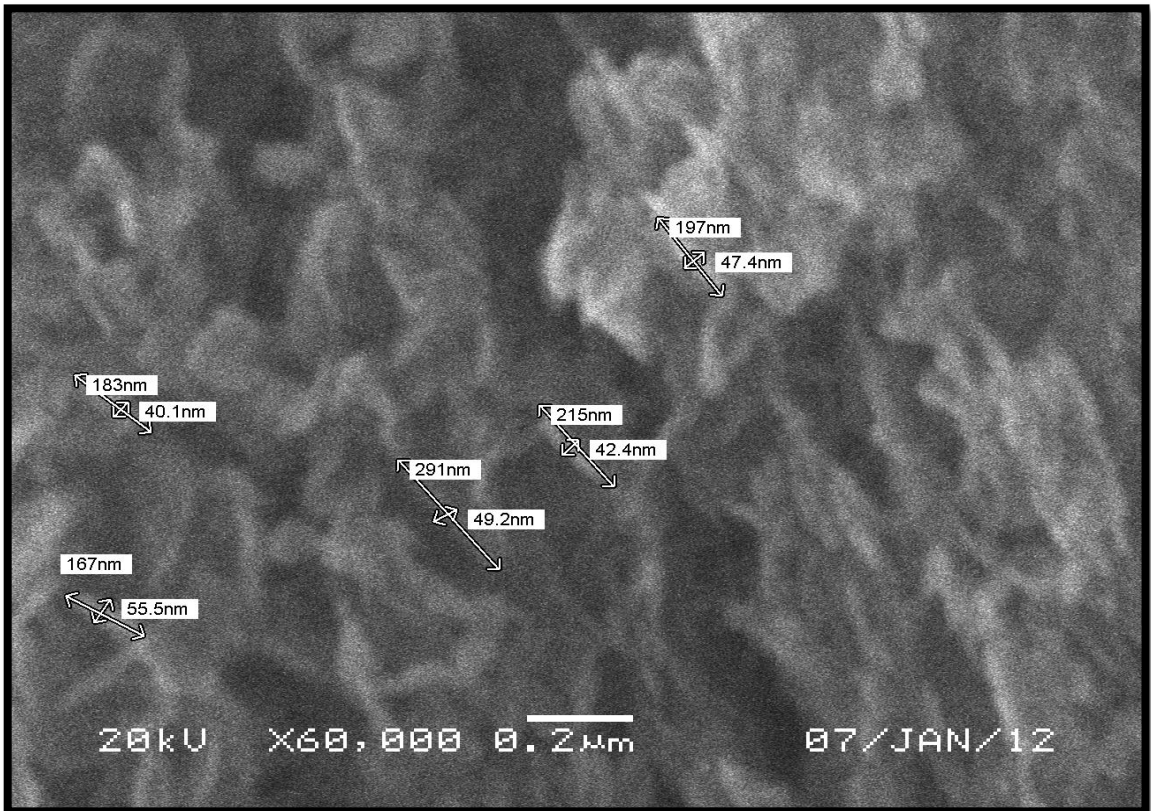


Figure 4.10: SEM for Sample 4.

For sample 5 that is prepared with TOAB stabilizer at 90 °C temperature, the SEM measurement shows that the samples are nanorods with length in the range 160-250 nm and width in the range 40-50 nm as shown in figure 4.11.



Figure 4.11: SEM for Sample 5

figures 4.9, 4.10, and 4.11 reveal blowzy shape of the irregular particle. No spherical particles were detected due to the surfactant effect, or type concentration, or thermodynamic of particles were affected by temperature. The results of the size of the samples from SEM analysis (length and width) are presented in table 4.2.

Table 4.2. The size of samples at different temperatures.

Sample No. For Cobalt Oxide	Stabilizer	Temp. Preparation	Length	Width
1	No	40 °C	260 μm	120 μm
2		90 °C	390 μm	230 μm.
3	PVP	40 °C	150-170 nm	40-50 nm
4		90 °C	160-250 nm	40-50 nm
5	TOAB	90 °C	160-250 nm	40-50 nm

Table 4.2 illustrates the effect of temperature, by increasing the temperature throughout synthesis the particles are effected in shape and size. It shows that the size increases with increasing the temperature at which the synthesis of the nanoparticles was performed. This result is in good agreement with Shalini *et al.*, 2012 work. They found that the size of silver nanoparticle was 10 NM for sample which was synthesized at 4 °C, and 20 nm for the sample which was synthesized at 50 °C.

This can be interpreted through the fact that by increasing the temperature, the random collision increases and the reactant consumption also increases, and this cause an increase in the growth and agglomeration process, resulting in larger particle size.

In this work, the results show that the presence of the stabilizer also affects the size of the obtained particles. In general, the presence of stabilizer prevents further agglomeration and hence results in smaller particle size.

The results of this work also show that smaller nanoparticles in nano range could be obtained in the presence of stabilizer in agreement with Upendra

et al., 2011 results. They found that the size decreases as the concentration of the PVP increases. Moreover, the results show that stabilizer type does not affect the size of the sample.

4.1.4 Vibrating Sample Magnetometer Magnetic Measurements

The VSM magnetic measurements for samples that were prepared without any stabilizer (micrometer size) are presented in figures 4.12 and 4.13 for samples 1 and 2, respectively. They show clear linear M-H curve which leads to a paramagnetic behavior. Because the atoms in paramagnetic materials play the role in this material, so $k_B T$ is comparable to KV' . Therefore, the graph of M versus H is linear. figures 8 and 9 in appendix B show that samples 1 and 2 didn't have superparamagnetic component.

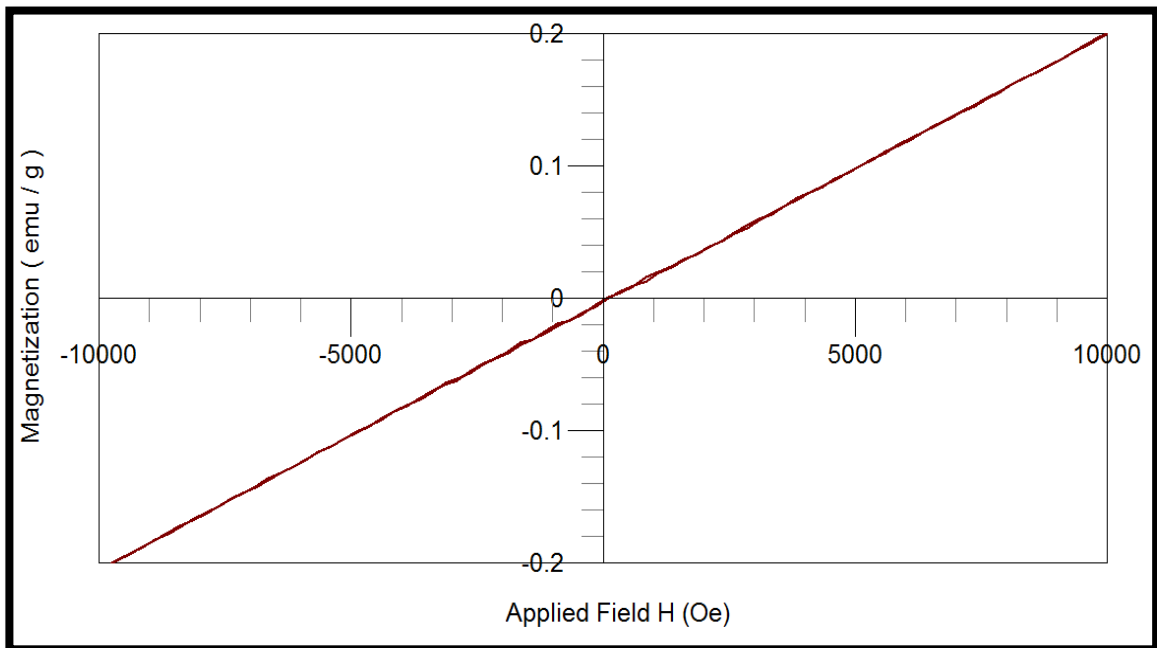


Figure 4.12: The magnetization curve at room temperature for sample 1, prepared without stabilizer at 40 °C.

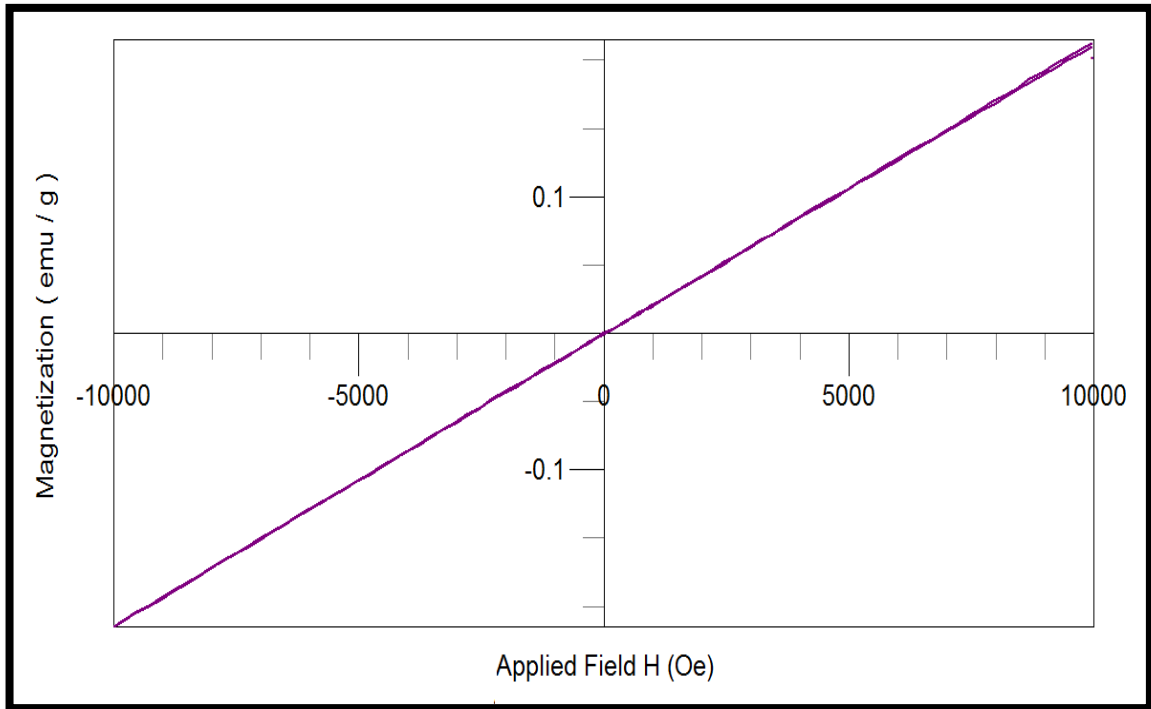


Figure 4.13: The magnetization curve at room temperature for sample 2, prepared without stabilizer at 90 °C.

The measured magnetized curve is presented in figures 4.14, 4.15 and 4.16, respectively for the samples 3, 4, and 5 that were prepared with stabilizer PVP and TOAB. The results showed a paramagnetic and small superparamagnetic behavior which may arise from clusters of thousands of atoms. This agrees with the work of Yang *et al.*, 2004. In his work, the sample of cobalt nanoparticles was prepared with Triphenylphosphine (TPP) surfactant stabilizer and showed no hysteresis curve, indicating a superparamagnetic behavior.

Superparamagnetic materials have clusters of atoms or particles and $K_B T$ is not comparable to KV' . Therefore, M vs. H curve behavior is nonlinear.

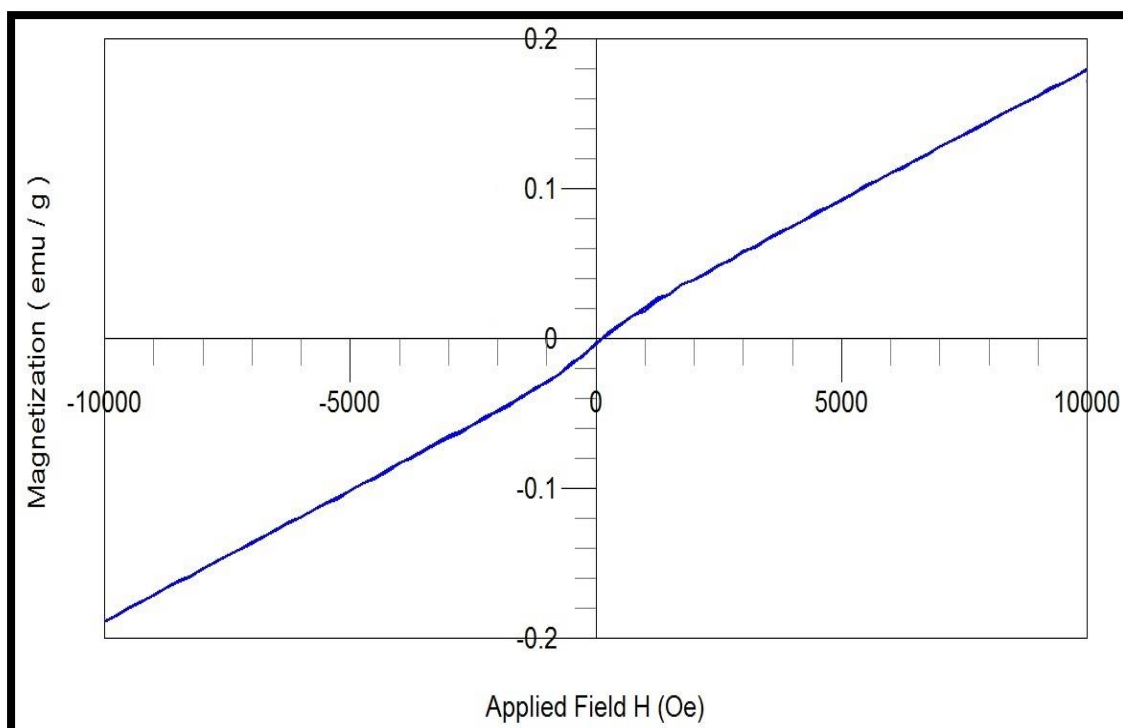


Figure 4.14: The magnetization curve at room temperature for sample 3, prepared with PVP stabilizer at 40 °C.

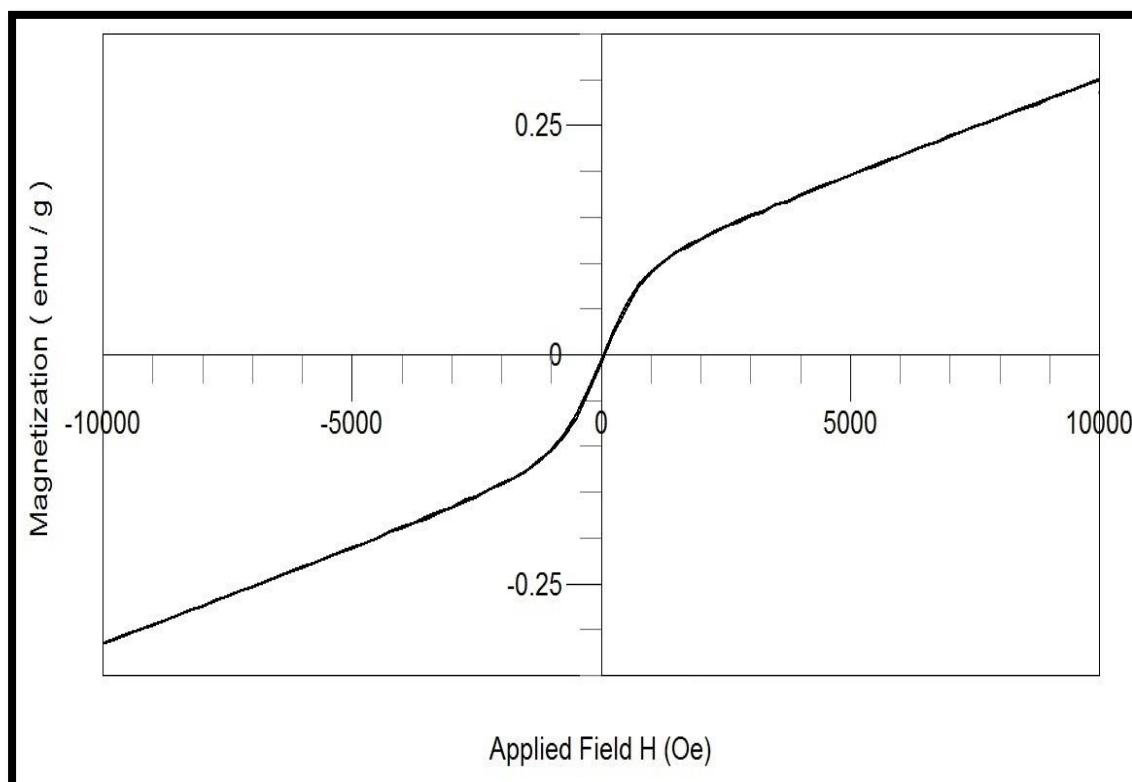


Figure 4.15: The magnetization curve at room temperature for sample 4, prepared with PVP stabilizer at 90 °C.

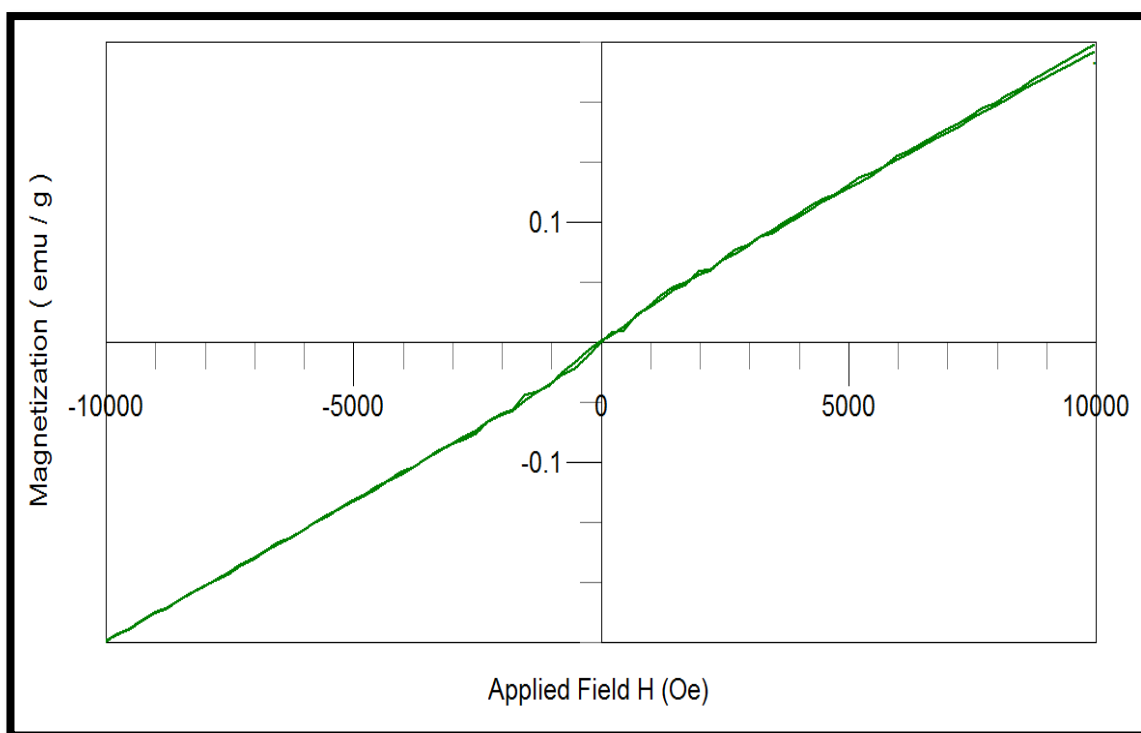


Figure 4.16: The magnetization curve at room temperature for sample 5, prepared with TOAB stabilizer at 90 °C.

The only superparamagnetic component of M-H curves for sample 3, 4, and 5, respectively, is presented in figures 4.17, 4.18, and 4.19 .

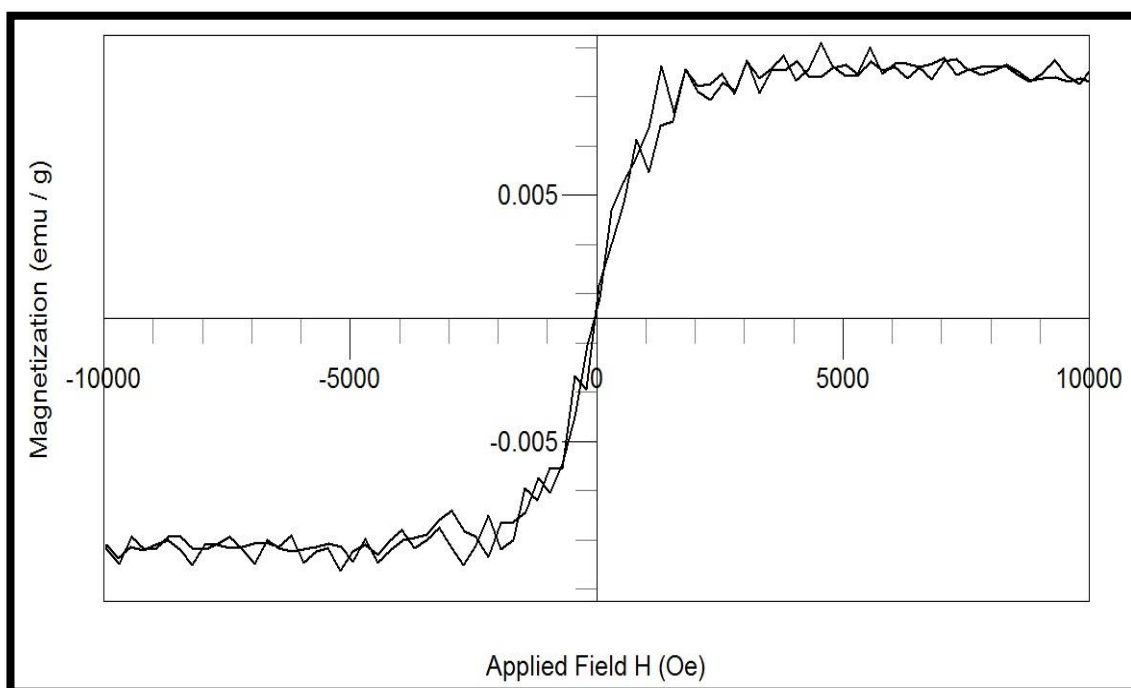


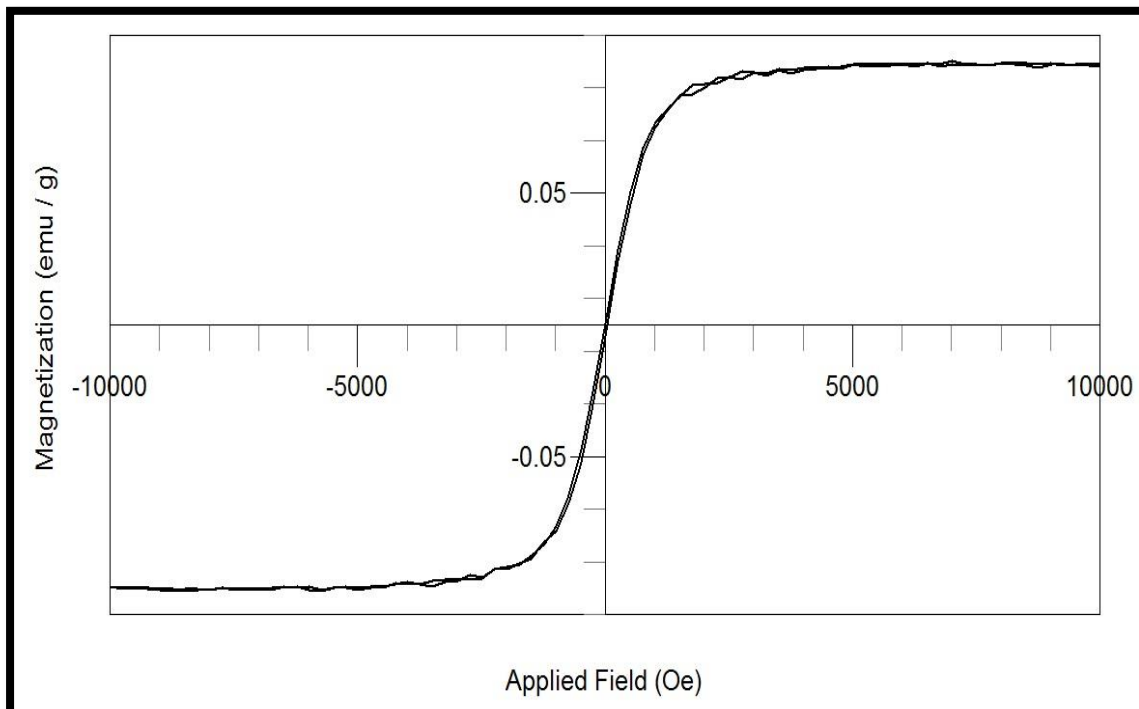
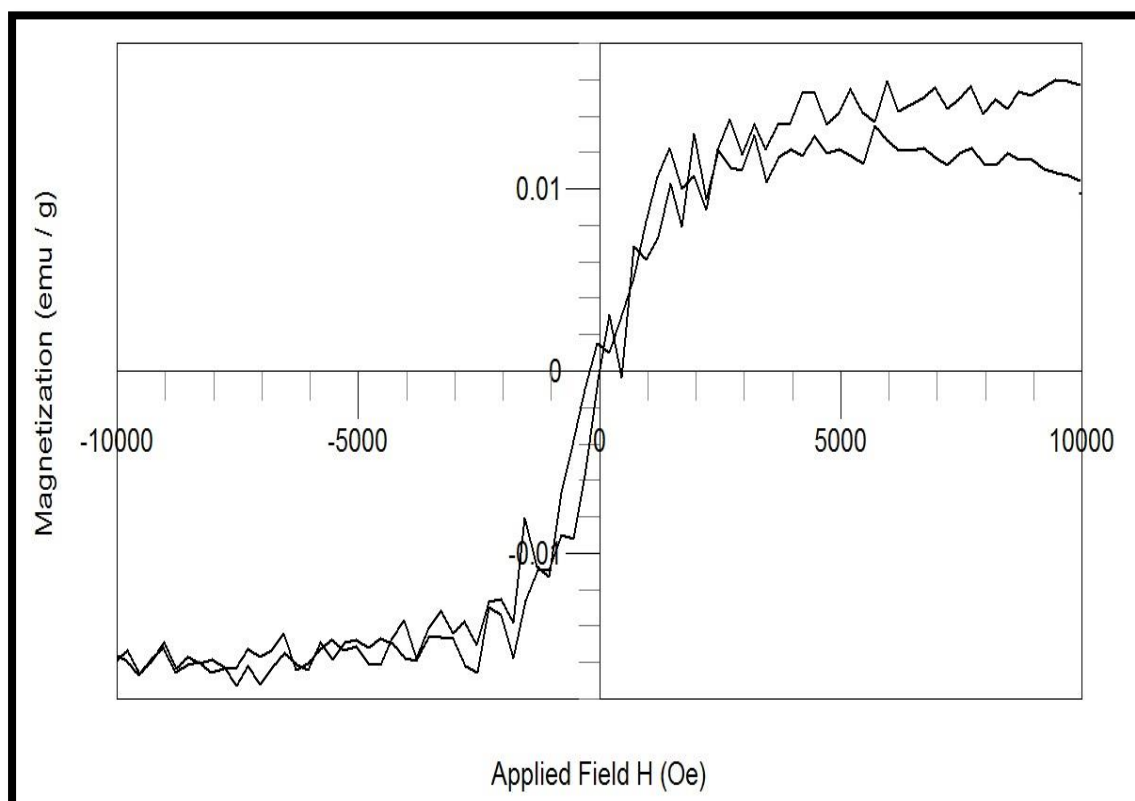
Figure 4.17: Superparamagnetic component of sample 3.**Figure 4.18:** Superparamagnetic component of sample 4.

Figure 4.19: Superparamagnetic component of sample 5.

The sample prepared with TOAB stabilizer shows weak superparamagnetic (figure 4.19), while sample prepared with PVP stabilizer shows a stronger superparamagnetic component (figure 4.18).

The superparamagnetic component of the sample is affected by stabilizer type used.

4.2 Conclusion:

In this study, the results show that there was no chloride present in the prepared samples, because it was completely oxidized to form Co-O. SEM measurements show that the size of the sample that were prepared without stabilizer are in the micro sized and the samples prepared with stabilizer are nanosized samples. The existence of stabilizer encapsulate atoms, which prevent agglomeration and thus get a smaller size, while the type of the stabilizer does not affect the size of the sample, which is in a good agreement with the results of Upendra *et al.*, 2011, who found that the size decreases as the concentration of the PVP increases. The size of the particles increases as the preparation temperature increases, which is in a good agreement with the result of Shalini *et al.*, 2012. They found that the size of silver nanoparticle was 10 nm, and 20 nm for the samples synthesized at 4 °C and 50 °C, respectively.

The measured magnetization curve for the sample that was prepared without any stabilizer (μm size) show clear paramagnetic behavior. However the measured magnetized curve for the sample that was prepared with stabilizer (PVP or TOAB) show paramagnetic with superparamagnetic

component, which agrees with the work of Yang *et al.*, 2004. They found that the samples of cobalt nanoparticles that were prepared with Triphenylphosphine (TPP) surfactant stabilizer show no hysteresis curve, indicating a superparamagnetic behavior. The magnetic property of samples depend on the size of the particles. Therefore, superparamagnetic behavior appears on the nanorods samples beside the paramagnetic behavior.

The stabilizer type affects the superparamagnetic component of the sample. While the samples which were prepared with TOAB stabilizer show weak superparamagnetic component, samples prepared with PVP stabilizer show stronger superparamagnetic component.

4.3 Future Work

- For non-stabilized samples there was absorption of carbon dioxide. Therefore, this opens the possibility for the use of these samples as gas sensors of carbon dioxide.
- Study the effect of different sizes on the magnetic property.
- Stabilize the samples with different stabilizers, and study of their impact on the size and magnetic property.
- Improving the preparation conditions to obtain smaller size .

References

1. Alberto Naranjo, Tim A. Osswald, Juan Diego Sierra, Marfa del Pilar Noriega, and Alejandro Roldan-Alzate, "**Plastics Testing and Characterization Industrial Applications**". German, Hanser Verlag. 363. (2008).
2. Al-Tuwirqi Reem M., Al-Ghamdi A.A., Al-Hazmi Faten, Alnowaiser Fowzia, Al-Ghamdi Attieh A., Abdel Aal Nadia, and El-Tantawy Farid, "**Synthesis and physical properties of mixed Co₃O₄/CoO nanorods by microwave hydrothermal technique**". Superlattices and Microstructures, **50**, 437–448, (2011).
3. Aslam M., Bhoje R., Alem N., Donthu S., and Dravid V. P., "**Controlled large-scale synthesis and magnetic properties of single-crystal cobalt nanorods**". Journal of applied physics, **98**, 074311 , 1-8, (2005).
4. Bandyopadhyay A. K., "**Nano Materials**". New Delhi, New age international (p) limited, publishers, 169, (2008).
5. Bean C.P. and Livingston J.D., "**Appl.Phys**". **30**, 120, (1959).
6. Chih-Wei Tang, Tsann-Yan Leu, Wen-Yueh Yu, Chen-Bin Wang, and Shu-Hua Chien, "**Characterization of cobalt oxides studied by FT-IR, Raman, TPR and TG-MS**". Taiwan, **48**, 267-274, (2004).
7. Chikazumi S., "**Physics of Magnetizm**". John Wiley and Sons Inc, New York, (1964).
8. Cullity B.D., "**Introduction to magnetic particles**". Addison – Wesley, New York, (1972)

9. Denny D. Tang and Yuan-jen Lee, "**Magnetic Memory Fundamentals and Technology**". United States Cambridge University Press, 208, (2010).
10. Dobrzański L., Drak M., Ziębowicz B., "**Materials with specific magnetic properties**". Journal of Achievements in Materials and Manufacturing Engineering, **17**, Issue 1-2, (2006).
11. Faraji M., Yamini Y., and Rezaee M., "**Magnetic Nanoparticles: Synthesis, Stabilization, Functionalization, Characterization, and Applications**". Iran, Chem. Soc, 7, (2010).
12. Frank A. Settle, "**Handbook of Instrumental Techniques for Analytical Chemistry**". New Jersey, Prentice Hall, 995, (1997).
13. Gubin S. P., Koksharov Yu. A., Khomutov G. B., Yurkov G. Yu., "**Magnetic nanoparticles: preparation, structure and properties**". Russian Chemical Reviews, **74** (6), 489 – 520, (2005).
14. Jianchun Bao, Zheng Xu, Jianming Hong, Xiang Ma, and Zuhong Lu, "**Fabrication of cobalt nanostructures with different shapes in alumina template**". Scripta Materialia, **50**, 19–23, (2004).
15. Jiangong Li, Yong Qin, Xinli Kou, Haiying He, Dakang Song, "**Structure and magnetic properties of cobalt nanoplatelets**". Materials Letters, **58**, 2506– 2509, (2004).
16. Karimian R., Zandi M., Shakour N., Piri F., "**Synthesis and characterization of manganese oxide and cobalt oxide nano-structure**". Journal of Nanostructures, JNS, **1**, 39-43, (2012).

17. Mathias Getzlaff, "**Fundamental of Magnetism**". Berlin, Springer, 378, (2008).
18. Min Nie, Kai Sun, and Dennis Desheng Meng, "**Formation of metal nanoparticles by short-distance sputter deposition in a reactive ion etching chamber**". *J. App. Phys.*, **106**, 054314, (2009).
19. Ming He, and Toh-Ming Lu, "**Metaldielectric Interfaces in Gigascale Electronics Thermal and Electrical Stability**". New York, Springer, 149, (2012).
20. Murugesan R., "**Electricity and Magnetism**". India, S. Chand & Company Ltd., 247, (2008).
21. Narayanan T. N., Shaijumon M., Ajayan P. M., and Anantharaman M. R., "**Synthesis of High Coercivity Core–Shell Nanorods Based on Nickel and Cobalt and Their Magnetic Properties**". *Nanoscale Res Lett*, **5**, 164–168, (2010).
22. Nee'l L., "**Ann. Geophys**". **5**, 99, (1949).
23. Pamela Alex, Sanjib Majumdar, Jugal Kishor, Inderkumar G. Sharma, "**Synthesis of Cobalt Nano Crystals in Aqueous Media and Its Characterization**". *Materials Sciences and Applications*, **2**, 1307-1312, (2011).
24. Paul Derry, and Andrew R. Barron, "**Physical Methods in Chemistry and Nano Science**". Texas, Rice University, 694. (2012).
25. Pauline S. and Persis Amaliya A., "**Size and Shape Control Evaluation of Cobalt (Co) and Cobalt Ferrite (CoFe₂O₄)**".

- Magnetic Nanoparticles"**. Archives of Physics Research, **3** (2),78-83, (2012).
- 26.Poddar P., Lwilson J., Srikanth H., Morrison S. A. and Carpenter E. E., "**Magnetic properties of conducting polymer doped with manganese–zinc ferrite nanoparticles**". *Nanotechnology*, **15**, S570, (2004).
- 27.Princeton Measurements Corporation, "**MicroMag™ 3900 VSM Magnetometer**". [Instruction Manual]. Princeton Measurements Corporation, New Jersey, United States, (2009).
- 28.Roa Baerga, and Victor Orlando, "**Laser shockwave sintering of micro and nanoscale powders of yttria-stabilized zirconia**". Ames, Iowa Graduate Theses and Dissertations, 11843, (2010).
- 29.Robert W. Kelsall, Ian W, Hamley. And Mark Geoghegan, "**Nanoscale Science and Technology**". England, John Wiley & Sons Ltd, 456, (2004).
- 30.Roman Boca, "**Theoretical Foundations of Molecular Magnetism**". Lausanne, Switzerland, Elsevier Science S.A., 874, (1999).
- 31.Shah M. A., "**Principles of Nanoscience and Nanotechnology**". India, Narosa Publishing House, 199, (2010).
- 32.Shalini Chauhan and Mukesh Kumar Upadhyay, "**Fruit based synthesis of silver nanoparticles-an effect of temperature on the size of Particles**". India, Recent Research in Science and Technology, **4**(5), 41-44, (2012).

33. Shihua Wu, Shoumin Zhang, Weiping Huang, Juan Shi and Baoping Li., "**Characterization and Magnetic Properties of Cobalt Nano-Particles Prepared by Metal Vapor synthesis Technique**". *J. Mater. Sci. Technol.*, **19**, No.5, 422-424, (2003).
34. Tahir Mehmood Awan, "**Studies of material parameters of magnetic materials**". *Stockholm, Sweden, KTH Electrical Engineering*, 50, (2008).
35. Upendra N. Tripathi, Ajay Soni, V. Ganesan, and Gunadhor S. Okram, "**Influence of polyvinylpyrrolidone on particle size of Ni nanoparticles preparation**". India, *AIP Conf. Proc.*, **1447**, 437-438, (2011).
36. Walter Benenson, John W. Harris, Horst Stocker, and Holger Lutz, "**Handbook of Physics**". New York: Springer, 1186, (2002).
37. Wei Wu Quanguo, and He Changzhong Jiang, "**Magnetic Iron Oxide Nanoparticles: Synthesis and Surface Functionalization Strategies**". *Nanoscale Res Lett*, **3**(11), 397–415, (2008).
38. William D. and Callister, Jr, "**Fundamentals of Materials Science and Engineering**". United States of America, John Wiley & Sons, 1619, (2001).
39. Wolfgang Nolting, and Anupuru Ramakanth, "**Quantum Theory of Magnetism**". Berlin Heidelberg: Springer, 752, (2009).
40. Yang H. T., Su Y. K., Shen C. M., Yang T. Z. and Gao H. J., "**Synthesis and magnetic properties of e-cobalt nanoparticles**". Wiley InterScience Surf. Interface Anal, **36**, 155 – 160, (2004).

41. Yang L. W., Wu X. L.,a and Qiu T., "**Synthesis and magnetic properties of Zn_{1-x}CoxO nanorods**". Journal of applied physics, **99**, 074303 ,1-5,(2006).
42. Yue Zhang, Zhi Yang , DiYin , Yong Liu, ChunLong Fei, Rui Xiong, Jing Shi, and GaoLin Yan, "**Composition and magnetic properties of cobalt ferrite nano-particles prepared by the co-precipitation method**". Journal of Magnetism and Magnetic Materials, **322**, 3470–3475, (2010).

Appendices

Appendix A

The procedure of analyzing and drawing VSM results using easy plot program is explained as the following:

For sample 3, for example, the raw data moment (in emu) vs. applied field H were plotted as shown in figure 1.

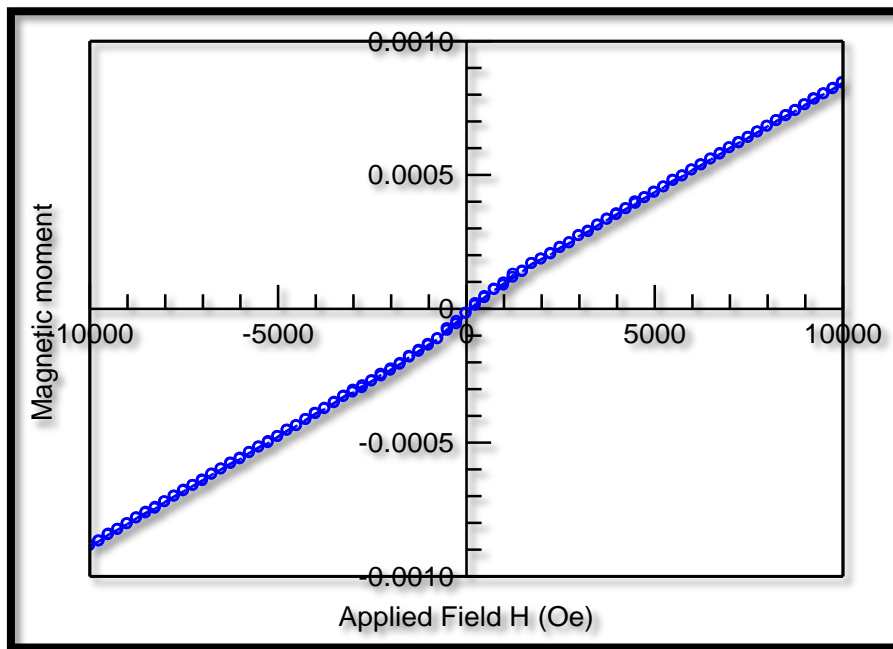


Figure 1: Magnetic moment versus applied field.

Then data moment divided by the mass (g) to get magnetization (emu/g), and Magnetisation vs. H were plotted as shown in figure 2.

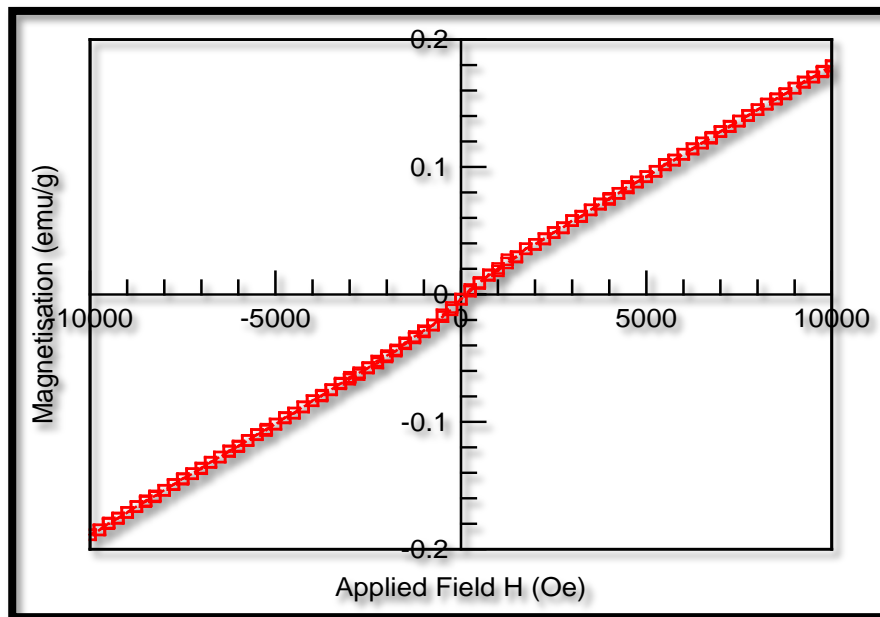


Figure 2: Magnetization versus applied field.

The high field in the positive region is fitted to a line (paramagnetic) and that in the negative region also is fitted to a line as shown in figure 3.

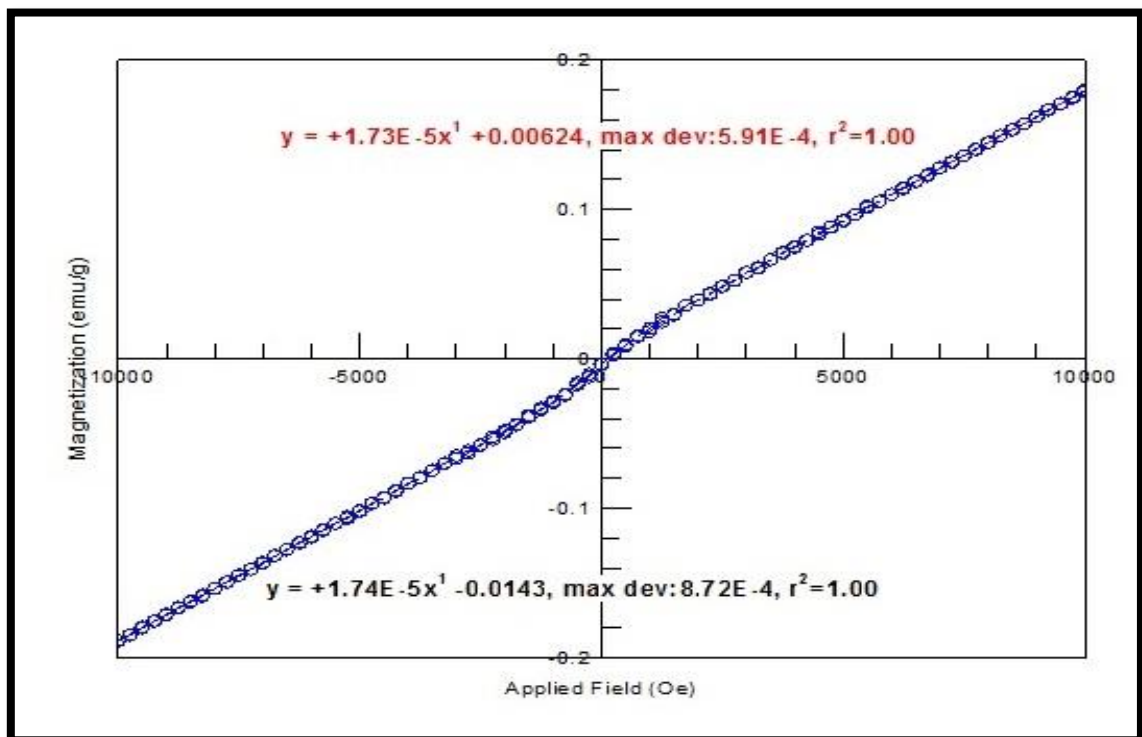


Figure 3: fitted positive and negative region to a line to get paramagnetic susceptibility.

The paramagnetic susceptibility is 1.735×10^{-5} emu/g.Oe at room temperature ($T=20^\circ\text{C}$). By removing this component, using transformation equation $y=y-1.735 \times 10^{-5} \times x$ as shown in figure 4. The superparamagnetic component will be obtained as shown in figure 5.

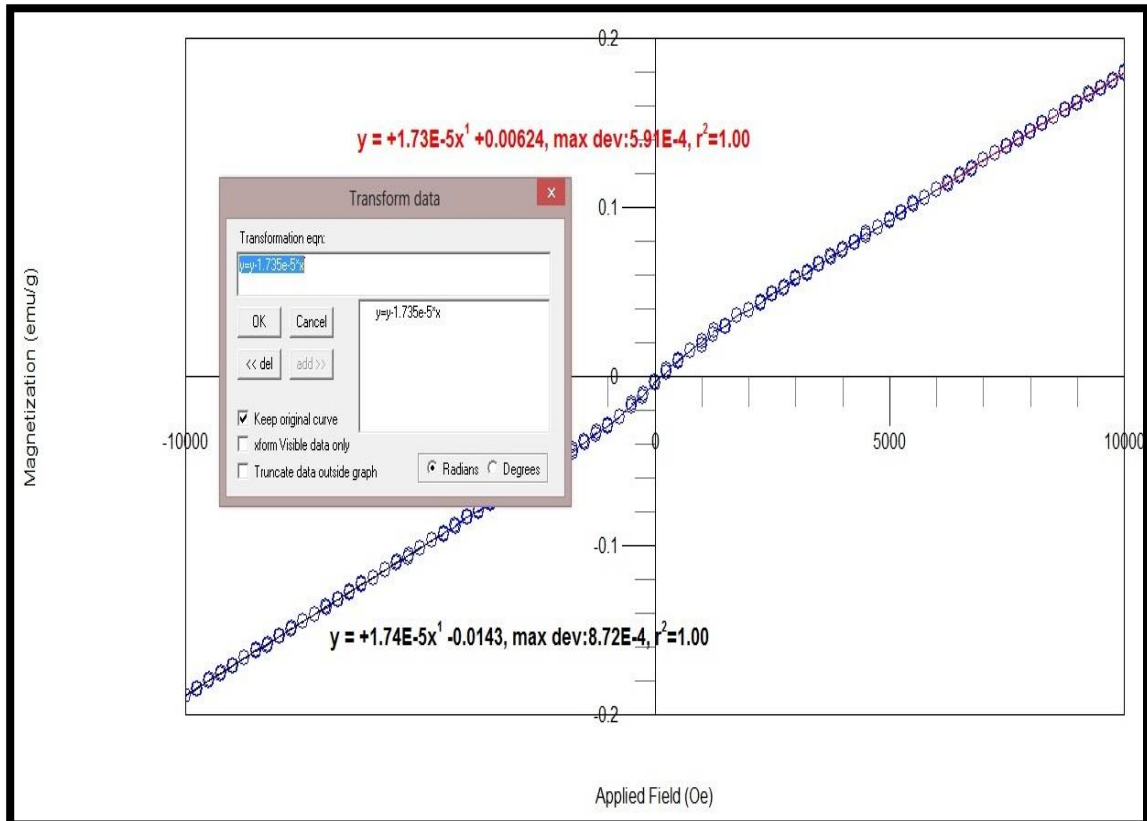


Figure 4: using transformation equation to remove paramagnetic susceptibility and get superparamagnetic component.

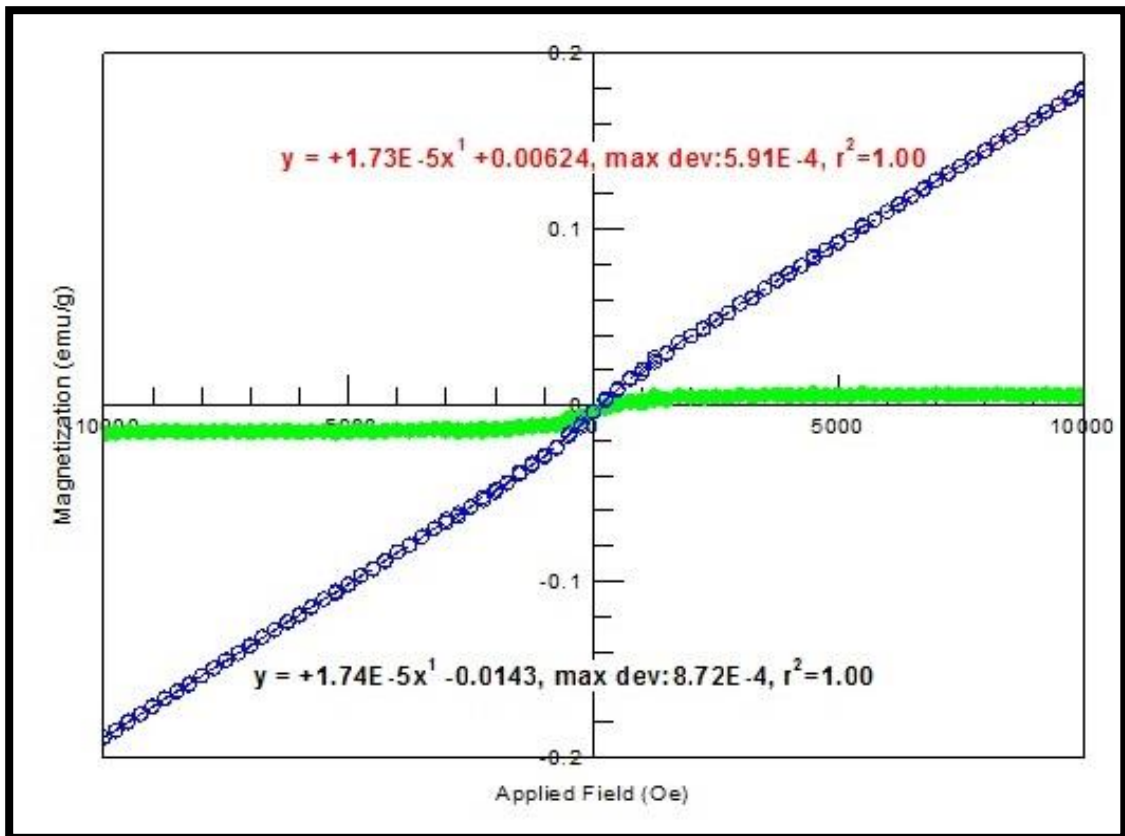


Figure 5: Magnetization versus applied field.

In figure 5 the new curve that appear is the superparamagnetic component of the sample. By deleting the total magnetization curve (superpara+para) the original curve, the only superparamagnetic behavior like S-shape shown in figure 6 .

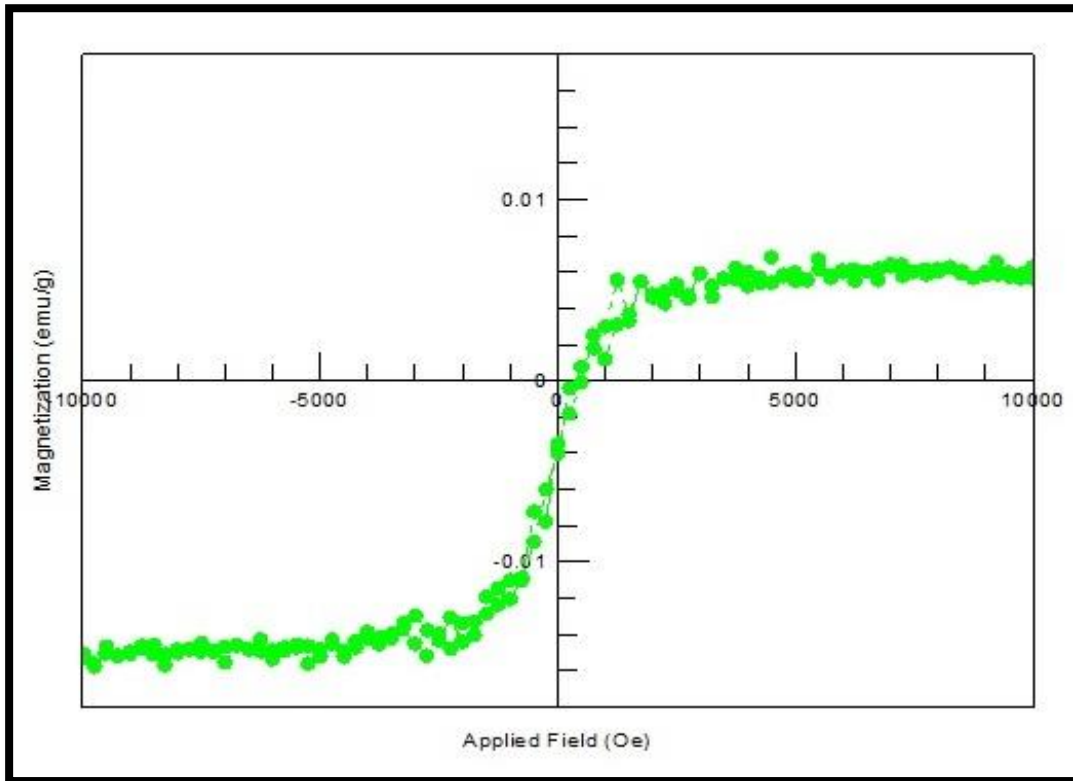


Figure 6: Magnetization versus applied field.

Then moving the curve since M_s and $-M_s$ are the same, as in figure 7.

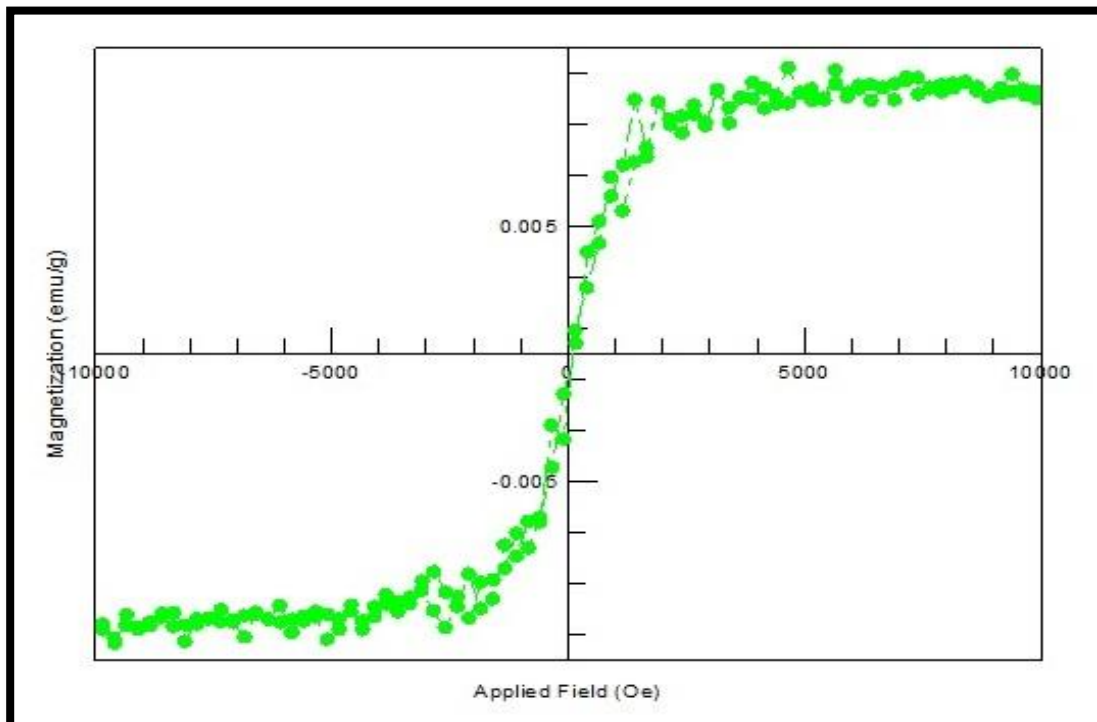


Figure 7: Magnetization versus applied field after treatment since M_s and $-M_s$ are the same.

Appendix B

The following figures (8 and 9) show that the samples do not have a superparamagnetic behavior, and figures (10, 11, and 12) show that the samples have a superparamagnetic behavior.

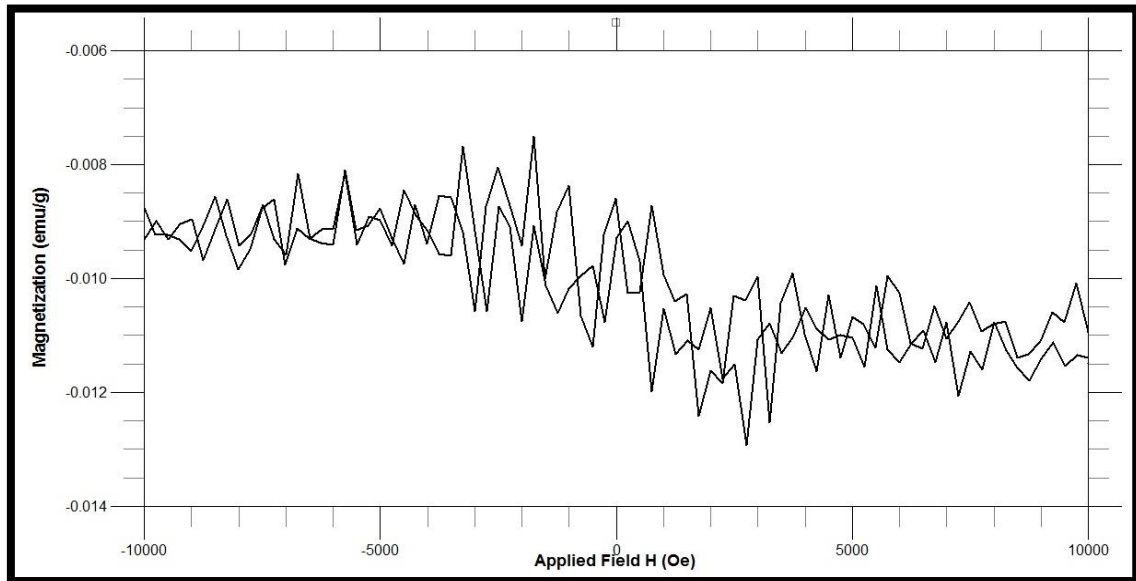


Figure 8: Magnetization versus applied field for sample 1 after removing paramagnetic component.

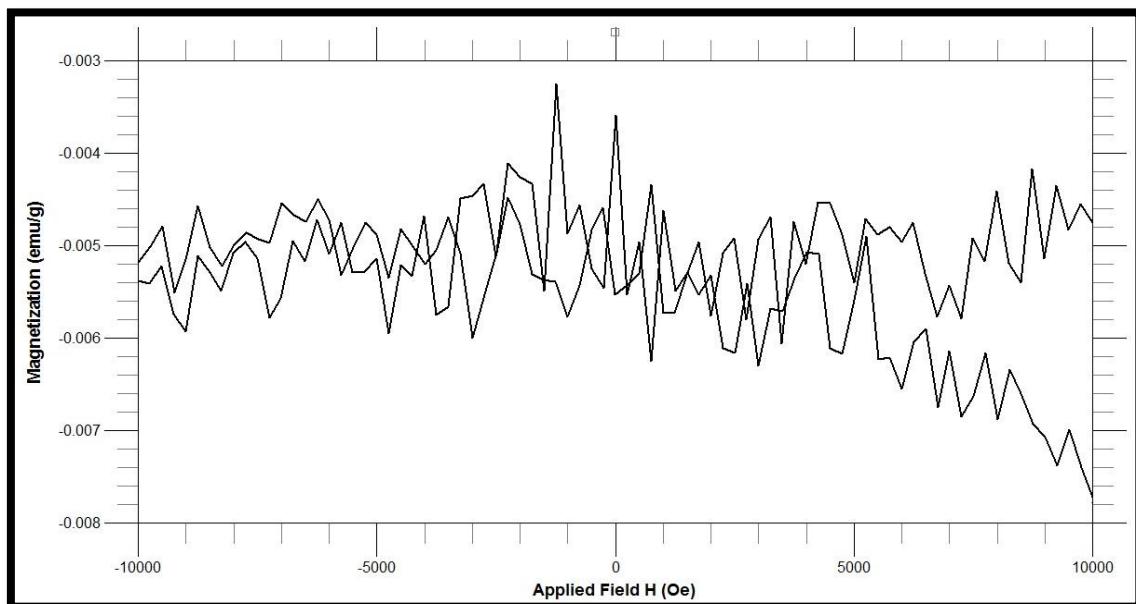


Figure 9: Magnetization versus applied field for sample 2 after removing paramagnetic component.

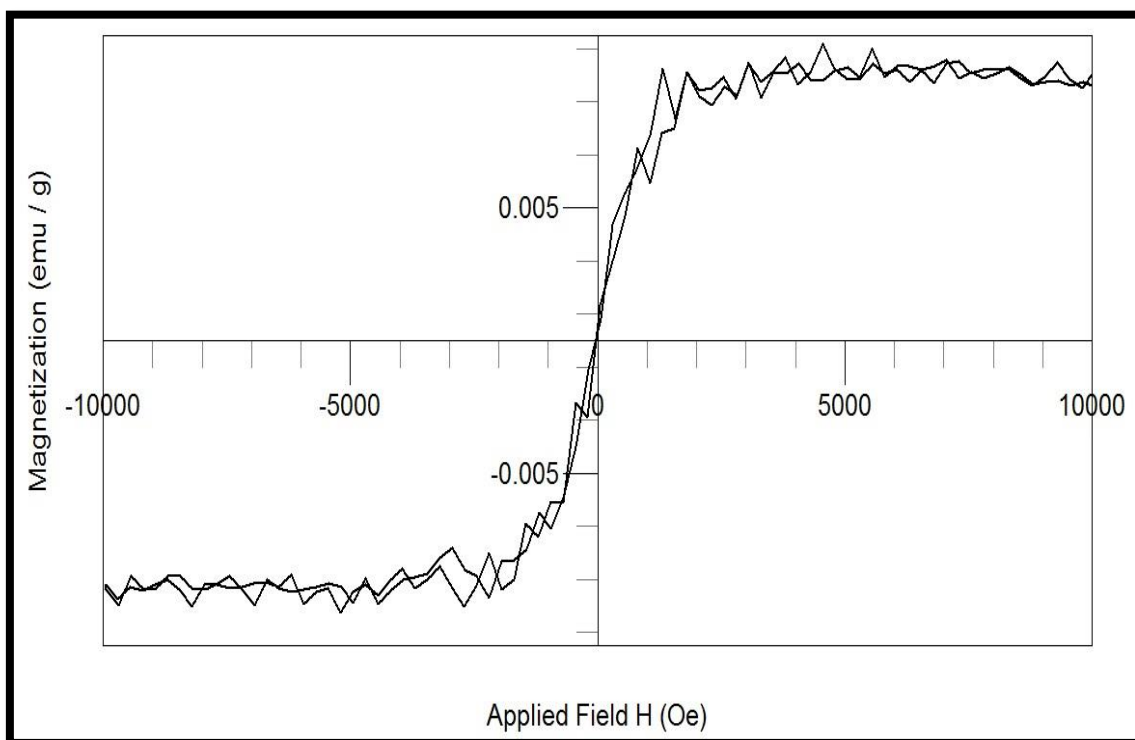


Figure 10: Magnetization versus applied field of sample 3, after removing paramagnetic component.

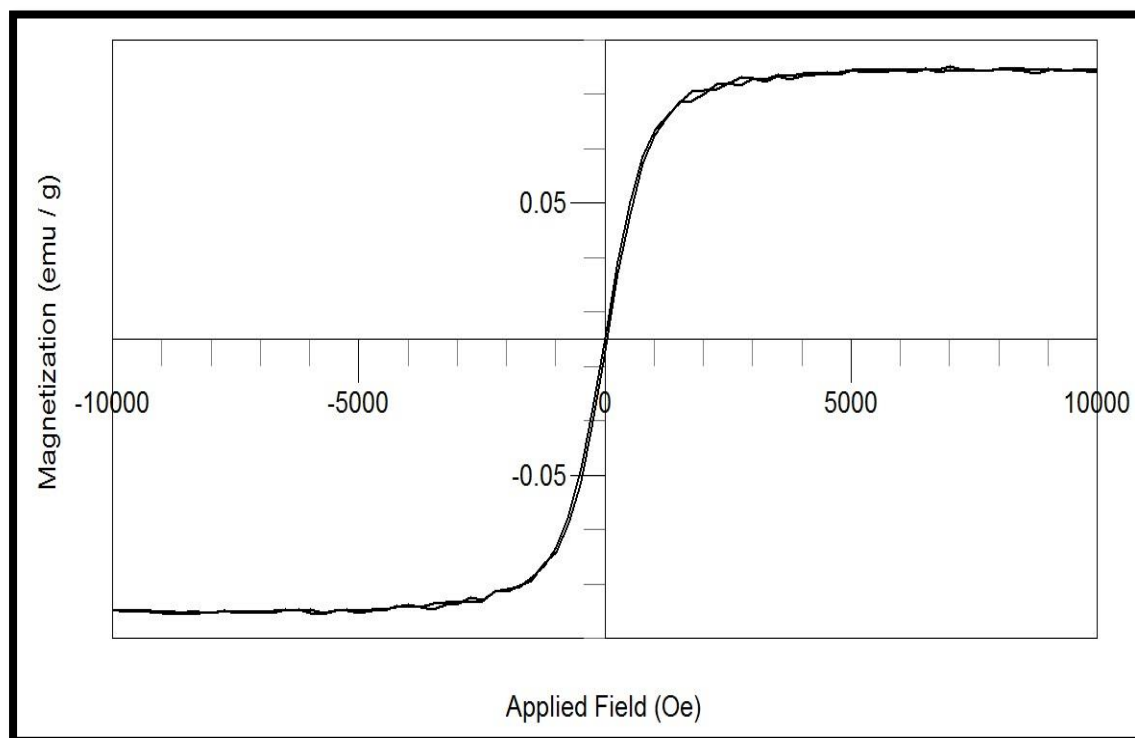


Figure 11: Magnetization versus applied field of sample 4, after removing paramagnetic component.

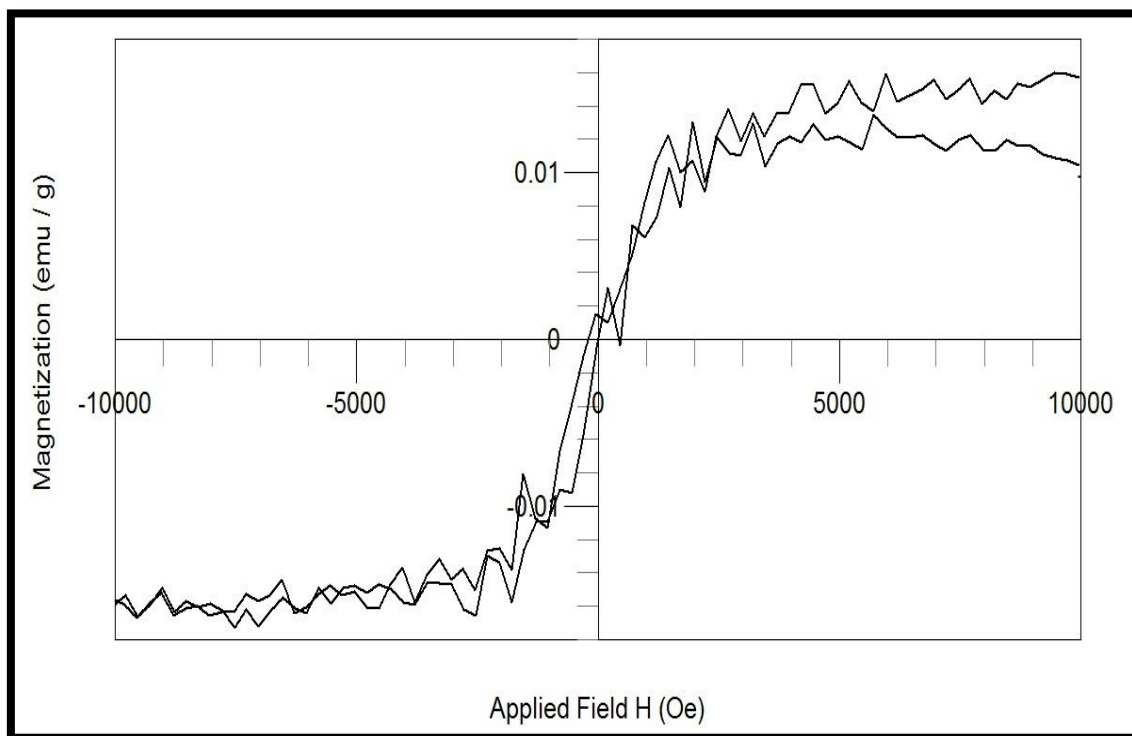


Figure 12: Magnetization versus applied field of sample 5. after removing paramagnetic component.

جامعة النجاح الوطنية
كلية الدراسات العليا

تحضير عينات من أكاسيد الكوبالت على شكل جزيئات نانوية ودراسة
خصائصها المغناطيسية

إعداد

فادي محمد مصطفى نعالوة

إشراف

د. شريف مسامح

د. محمد سليمان

قدمت هذه الأطروحة استكمالاً لمتطلبات الحصول على درجة الماجستير في الفيزياء بكلية
الدراسات العليا في جامعة النجاح الوطنية في نابلس - فلسطين.

2013 م

ب

تحضير عينات من أكاسيد الكوبالت على شكل جزيئات نانوية ودراسة خصائصها المغناطيسية

إعداد

فادي محمد مصطفى نعالوة

إشراف

د. شريف مسامح

د. محمد سليمان

الملخص

في هذه الدراسة تم تحضير عينات مختلفة الحجم من أكاسيد الكوبالت باستخدام طرق كيميائية حيث تم استخدام طريقة اختزال الملح، على درجات حرارة مختلفة وبإضافة نوعين مختلفين من أنواع المثبت PVP و TOAB.

وجد أن العينات التي كانت تحتوي على مثبت كان حجمها صغير في حجم النانو، بينما التي كانت لا تحتوي على مثبت كانت في حجم الميكرو. نوع المثبت المستخدم لم يكن له تأثير على الحجم.

وتبين كذلك من هذه الدراسة أن درجة الحرارة المستخدمة أثناء التحضير تؤثر على الحجم، حيث أن الحجم يزداد بزيادة تلك الدرجة.

العينات التي لا تحتوي على أي نوع من المثبت أظهرت النتائج أنها عبارة عن paramagnetic، والعينات التي تحتوي على المثبت بنوعيه ذات الحجم النانوي عبارة عن paramagnetic with superparamagnetic.

الخصائص المغناطيسية تتأثر بنوعية المثبت، حيث أن المثبت من نوع PVP كانت فيه superparamagnetic component أقوى من المثبت من نوع TOAB.